Benchmarking proton exchange membrane fuel cell cathode catalyst at high current density: a comparison between the rotating disk electrode, the gas diffusion electrode and differential cell

Raphaël Riasse, Clémence Lafforgue, Florent Vandenberghe, Fabrice Micoud, Arnaud Morin, Matthias Arenz, Julien Durst, Marian Chatenet

Benchmarking proton exchange membrane fuel cell cathode catalyst at high current density: a comparison between the rotating disk electrode, the gas diffusion electrode and differential cell

Raphaël Riasse[1-2], Clémence Lafforgue[1,3], Florent Vandenberghe[1,3], Fabrice Micoud[3], Arnaud Morin[3], Matthias Arenz[4], Julien Durst[2] and Marian Chatenet[1]

[1] *Univ. Grenoble Alpes, Univ. Savoie Mont Blanc, CNRS, Grenoble INP*, LEPMI, 38000 Grenoble, France*

[2] *Symbio, 5 Rue Simone Veil, 69200 Vénissieux, France*

[3] *Univ. Grenoble Alpes, CEA, LITEN, DEHT, F-38000 Grenoble, France*

[4] *Department of Chemistry, Biochemistry and Pharmaceutical Sciences, Univ. of Bern, Freiestrasse 3, 3012 Bern, Switzerland*

*Institute of Engineering and Management Univ. Grenoble Alpes

Abstract

The intrinsic activity of oxygen reduction reaction (ORR) electrocatalysts for proton exchange membrane fuel cell (PEMFC) is usually evaluated with the rotating disk electrode (RDE), an easy-to-use technique requiring little amount of electrocatalyst. However, the liquid environment of the RDE implies strong limitation of O_2 mass-transport and the intrinsic activity is only accessible on a narrow potential range (from 0.95 to 0.85 V *vs*. RHE) that is not relevant for the PEMFC operating conditions. This work compares results obtained with the RDE (0.2 cm²), the gas diffusion electrode (GDE, 0.07 cm²) and a small unit PEMFC (DC, 1.8 cm²). Three widely used ORR electrocatalysts are compared: Pt/Vulcan carbon, PtCo/Vulcan carbon and Pt/graphitized carbon, catalytic layers being prepared with a loading of 20 μg_{Pt} cm^{-2} and characterized at 25-30°C and full hydration. The results show that all setups have their own advantages and drawbacks. Regardless the electrocatalyst nature, the GDE allows to assess the intrinsic activities on a large potential range (from 0.9 to 0.6 V), in agreement with the results obtained in RDE for high potential and with the DC for lower potential. The GDE is therefore promising, enabling easy high current density measurements with little amount of electrocatalyst.

Keywords

Proton exchange membrane fuel cells (PEMFC); Oxygen reduction reaction (ORR); Platinum; Electrocatalyst; Rotating disk electrode (RDE); Gas diffusion electrode (GDE); Differential cell; intrinsic activity measurements; thin catalyst layer

Graphical Abstract

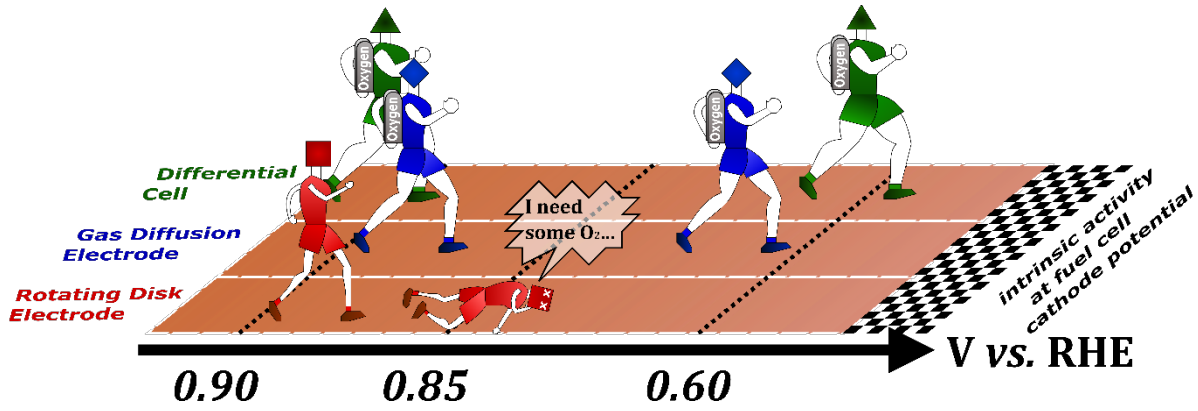

1. Introduction

It has become common knowledge that global warming is connected to a disastrous use of fossil energies since two centuries. Although downsizing our energy consumption would be the most efficient remedy, developing renewable energies is the main present target worldwide, which implies that the scientific community finds ways to efficiently store electricity, renewable sources being inherently intermittent. Among others, power-to-gas and in particular power-to-hydrogen is foreseen as a good manner to store renewable electricity, hydrogen being a versatile vector that can be used as raw chemical (reducer) in the industry, burned to generate heat or electrochemically converted back into water whilst producing electrical power in fuel cells [1]. In that latter case, proton exchange membrane fuel cells (PEMFCs) are by far the most advanced systems, and are therefore considered as a promising conversion system to decarbonize the current energy production mix, for (heavy and light) mobility or stationary applications. Many countries worldwide invest on research programs to develop renewable hydrogen production via water electrolysis and fuel cells, believing in their positive role for the ecological transition [2]. However, this kind of conversion devices rely mainly on the use of platinum group metals (PGM) to reach appropriate performance and durability, which questions the sustainability of the approach [3]. Indeed, the catalysts of present commercial systems are synthesized from PGM, the present endeavor being to improve the intrinsic activity and the operational stability of the designed catalysts. If one restricts to oxygen reduction reaction (ORR) catalysts that are used at PEMFC cathodes (ORR catalysts are one very critical component of these systems [4,5]), there are two mains routes that are employed nowadays to prepare "better" catalysts: structurally ordered or structurally disordered carbon-supported catalysts [6]. Both types of materials exhibit impressive "enhancement factors" over classical Pt/C catalysts, *i.e*. are far more intrinsically active than the latter for the ORR; this of course shall enable to improve the overall energy conversion of PEMFC, but, to date, these materials have never been appropriately employed in PEMFC cathodes and their use in real devices always ended up in disappointing performances [7]. This questions whether the methodology to characterize these "advanced catalysts" activity at the lab scale is relevant for applications or not.

The most-widely used tool to characterize one catalyst's ORR activity is the rotating disk electrode (RDE) setup. Present in (almost) every electrochemical laboratory, the RDE finds its popularity in the fact that it is simple and easy to use. RDE is actually employed to characterize PEMFC ORR (and HOR) catalysts since more than three decades. In particular, using a RDE is compatible with the characterization of small amounts of (Pt-based) catalysts (< 50 mg). This is an advantage, because PEMFC catalyst developers sometimes have difficulties to synthesize batches of their materials that are larger than a few mg, and direct PEMFC characterizations would hardly be feasible with such low amounts (or at least could not be reproduced and optimized in a reliable manner). Of course, the methodology to evaluate ORR catalysts in RDE has been deeply optimized over the years, which now leads to very robust and reproducible methodologies to properly benchmark Pt-based ORR catalysts [8–10], both in terms of initial performance and durability. After such initial benchmarking, the more promising catalysts can be upscaled, integrated in membrane electrode assembly (a procedure that is materials consuming [11–13]) and studied under real operating PEMFC conditions. However, the RDE

suffers from an inherent drawback when it comes to characterize reactions involving gaseous reactants (like those of PEMFC and the ORR in particular): the gas (here O_2) is transported to the catalyst interface whilst dissolved in the electrolyte, the solubility being small (*ca.* 1 mmol L^{-1}) and the diffusion coefficient also (*ca.* 10^{-6} cm^2 s^{-1}) [14]. This means that O_2 transport is roughly four decades slower than in the gas phase; this is why one observes diffusion-convection (mass-transport)-limited plateaus in RDE (with maximum current densities absolute values on the order of 5.5 mA cm^{-2} at 1600 revolution per minute (rpm) of the RDE, *i.e*. at least between two and three orders of magnitude smaller than classical current densities for PEMFC cathodes). Of course, one always tries to correct mass-transport (and Ohmic drop) limitations from RDE data, but the result of this correction becomes imprecise as soon as ORR potential values below 0.85 V *vs.* RHE are targeted (for state-of-the-art Pt-based catalysts). In other words, the RDE can only lead to a direct assessment of the catalytic activity above 0.85 V *vs.* RHE, which is not the region of interest for PEMFC cathodes, and at rather smaller current densities than in real PEMFC systems: the experimental conditions of the RDE forbid to access the catalytic performance in the same potential range as the one in a real PEMFC, and extrapolation must be made if ones wants to "predict" the behavior of a given catalyst in a PEMFC cathode, which is, of course, a large source of uncertainty. This also excludes all the work one must perform on the optimization of the ink formulation for the active layer preparation. The issue is even more important when the studied ORR catalysts are more active than the present state-of-the-art (so-called advanced catalysts presenting large enhancement factors), which is the present target of all catalyst developers in the PEMFC community.

The scientific community has gradually become aware of the intrinsic limitations of the RDE setup, and strived to overcome it. In the early 2000s, the group of Grenoble introduced the gas diffusion electrode (GDE) to benchmark PEMFC cathode catalyst [15,16], the idea relying on earlier works in the field of phosphoric acid fuel cell catalysis [17,18]. Then, the group of Kucernak at Imperial college, London, made several (mostly successful) attempts to unveil the kinetics of fast reactions in three-electrode cells using liquid electrolytes, with notably the so-called floating electrode setup [19–22]. However, the floating electrode has not been exported to other labs, yet, owing to difficulties in avoiding electrode flooding, related to the absence of convective flux at the vicinity of the active layer. The same drawback was experienced in the former version of the GDE used by Antoine *et al.* [15,16]. To cope with this limitation, Arenz *et al.* and Wilkinson *et al.* did recently revisit the GDE, and specifically modified the seminal setup so to incorporate gas channels that feed the studied active layer with a tightly-controlled convective flux, overall enabling to prevent the flooding of the active layer [23–25]. To make a long story short, these setups are compatible with operation at rather high current density for the ORR, making possible to approach the intrinsic catalytic activity (corrected from ohmic drop and mass-transport limitations) of a given catalyst in three-electrode cells in the potential region where it would be operated in a PEMFC cathode. From then on, studies flourished, where the GDE was used to test many catalysts, with the aim to demonstrate the relevance of the methodology to reach high electrode performance and assess catalytic durability [26–29]. Recently, one multiple-lab paper aimed to compare their respective GDE systems (and with RDE based-data) [30], while the group of Gasteiger

emphasized the advantages and limitations of RDE characterizations versus PEMFC characterizations [31]. While the former paper concluded that the way these GDE setups are used, they cannot deliver universal information (each GDE half-cell design come with its own advantages and limitations), the latter concludes that RDE also suffers limitations that prevent forecasting reliably one catalyst behavior in PEMFC (it also states that PEMFC measurements are not easy to benchmark catalysts). So, one must admit that, to date, there are still uncertainties in the propensity of non-PEMFC techniques to predict what performance a given catalyst will be capable to deliver in a real PEMFC, with special emphasis with ORR catalysts to be used in PEMFC cathodes. It is also commonly admitted that PEMFC testing may not be generalized for catalyst benchmarking, in view of the technological difficulties and tediousness associated to such characterizations (not to speak from the fact that if one wants to assess the intrinsic catalytic activity, one needs to make sure other limitations are appropriately corrected, a hard task for real PEMFC membrane electrode assemblies).

To cope with these difficulties, the present study aims to compare in a systematic manner three methodologies to assess the intrinsic catalytic activity of carbon-supported Pt-based ORR catalyst for PEMFC cathodes (**Figure 1**). The first is the RDE; the second is the GDE (using a setup resembling that of Arenz in Univ. Bern); the third is a small unit PEMFC (1.8 cm^2) operated in conditions where mass-transport shall be less-limiting (possible removal of liquid water through the membrane and no liquid electrolyte) and homogeneous in the surface of the active layer (high reactant stoichiometries), the so-called differential cell (DC). In all cases, because the objective is to determine the intrinsic activity of the catalysts, the aerial Pt-loading will be kept small (20 $\mu g\ cm^{-2}$), a value which is near-universally used for RDE characterizations, and which shall enable minimizing (if not ruling out) any mass-transport limitations in the thickness of the active layer (small loadings are also targeted by PEMFC developers). So, these three experimental setups are employed for the determination of the performances of a given catalyst in so-called model conditions (RDE), semi-model conditions (GDE) and close to real conditions (DC), in all cases with the objective to limit as much as possible the mass-transport limitations (and to correct them). This work focuses on three representative (and widely-used) ORR catalysts, provided by Tanaka Kikinzoku Kogyo (TKK): Vulcan XC72-supported Pt nanoparticles, Vulcan XC72-supported Pt_3Co alloyed nanoparticles and graphitized carbon-supported Pt nanoparticles. In this choice, the catalyst composition was varied at given carbon support (Pt and Pt_3Co on Vulcan XC72) or at given catalyst with varying carbon supports (Pt on Vulcan XC72 and on GC). Each of these materials are thoroughly characterized in the three experimental setups in conditions that are similar in terms of temperature and (when relevant) relative humidity, the markers of performance being the electrochemical surface area (ECSA) and the specific and mass activities (SA and MA, respectively), measured on the relevant potential interval for PEMFC cathodes (from 0.6 to 0.95 V *vs.* RHE). Furthermore, the study aims to determine (i) whether one technique is more relevant/reliable than the others to approach the intrinsic properties of the studied catalysts, (ii) whether the techniques are all equally usable for all the catalysts studied (depending on the Pt-based nanoparticles composition/morphology and the nature of the carbon support) and more generally (iii) to draw a clear picture about the advantages and drawbacks of the three techniques to benchmark PEMFC cathode catalysts.

2. Experimental

2.1. Catalyst materials

In this study, three different catalysts have been chosen to enable a multi-angle comparison of the experimental setups. All catalysts have been ordered from Tanaka Kikinzoku Kogyo (TKK) and are carbon-supported platinum or platinum alloyed nanoparticles: Vulcan XC72-supported Pt nanoparticles (Pt 47wt% on Vulcan XC72, TEC10V50E, noted Pt/XC72), Vulcan XC72-supported PtCo alloyed nanoparticles (PtCo 52wt% on Vulcan XC72, TEC36V52, noted PtCo/XC72) and graphitized carbon-supported Pt nanoparticles (Pt 30wt% on graphitized carbon, TEC10EA30E-HT, noted Pt/GC) powders have been used as received for the ink elaboration and the TEM grid preparation.

The particles morphology and distribution over the carbon support were investigated by transmission electron microscopy coupled with X-ray energy dispersive spectrometry (TEM-XEDS), and the corresponding (isolated) particle size distribution histograms were determined by measuring the diameter of at least 200 isolated particles for each catalyst on a minimum of 15 TEM pictures using the software ImageJ (**Figure 2**). The gold TEM grid was simply dipped into the catalyst's powders without any more complex preparation and imaged as such: electrostatic forces are enough to stabilize the particles on the grid. A Jeol 2010 TEM operated at 200 kV and equipped with elemental analysis (X-ray energy dispersive spectrometry, X-EDS, Oxford, INCA) was used for the observations.

2.2 Chemicals & Gases

Because the objective of this work is to measure the intrinsic activity of the three Pt-based catalysts, the experimental conditions needed to be as controlled (clean) as possible. To that goal, cleaning of all glassware and PTFE parts of the RDE and GDE cells, was made using a mix of 30 wt.% hydrogen peroxide (H_2O_2, Chem-Labs) and 96% sulfuric acid (H_2SO_4, Roth) in which the cells were soaked overnight to remove any organic pollution. Then, the cells were thoroughly rinsed with Ultrapure water (resistivity = 18.2 MΩ cm, total organic carbon (TOC) < 3 ppb) from a Milli-Q system (Millipore, Merck) - at least 2 rinsing for every component - and the cells were then boiled in water for at least 1 h before another rinsing to remove traces of (hydrogen)sulfate species, which are known to be strongly-adsorbed at Pt-based catalysts' surface.

Pure gases (Messer) were used for the RDE and GDE electrochemical measurements: Ar (99.999%), CO (99.997%), O_2 (99.999%). For characterization with the DC, gases from Air Product were used: N_2 (99.998%), H_2 (99.97%) and O_2 (99.995%). For the GDE and DC operation, a gas diffusion layer (GDL) with microporous layer (MPL) was used to immobilize the catalyst layer of the desired catalyst material, respectively a Freudenberg H23C8 and a Sigracet 22BB. A Nafion 115 (Dupont) membrane was used for the preparation of the DC membrane electrode assemblies (MEAs).

2.3. Catalyst Ink, electrode, electrolyte and cells

For the RDE setup, a glassy carbon rod of 5 mm diameter (section = 0.196 cm^2) was used as the working electrode; the counter electrode was a platinum mesh and a home-made reversible hydrogen electrode (RHE, reference electrode) was prepared daily with the same electrolyte and maintained at distance using a Luggin capillary. A platinum wire was placed in the cell as a fourth electrode and a capacitive bridge connects it to the reference electrode, this setup acting as a high-frequency-noise filter [32].

Prior to each active layer deposition, the glassy-carbon RDE tips were mirror polished (down to 1 µm, using diamond paste), and the polishing solvents removed in ultrasonic baths of 99.8% Acetone (Fisher Chemical), then 96% ethanol (EtOH, VWR Chemicals) and then water.

The RDE catalytic inks were prepared using a solution of ultrapure water and isopropanol (IPA, HPLC grade Fisher Chemical) with a volumetric ratio of H_2O:IPA = 2.5; a 5 wt.% Nafion®dispersion (1100EW, Sigma Aldrich) was used as a binder (the catalyst being mixed with ultrapure water and IPA and then Nafion in this order, for security reasons). The inks were then placed for 30 minutes in an ultrasonic bath filled initially with cold water (*ca.* 10°C). These inks were immobilized at the glassy-carbon RDE tips via spin-coating, using a methodology derived from that of Garsany *et al.* [10]. A dry fraction of platinum equal to 20 µg cm^{-2}_{geo} in a 10 µL ink volume was targeted. The tip was then heated to 90°C and the electrode was elaborated by drop-casting an aliquot of 10 µL on the rotating tip in a hot and convective air flow.

The electrolyte preparation was made with extremely pure reactants, here 70% perchloric acid ($HClO_4$, Suprapur Supelco Merck RDE // Rotipuran Ultra Roth GDE) and ultrapure water; 0.1 mol L^{-1} $HClO_4$ was used in the RDE setup. Overall, the configuration of the active layer in a RDE consists of a fully-flooded interface, through which the reactants (here O_2 and H^+) are transported in the liquid phase (**Figure 1** - A)

For the GDE cell, a modified version of the device of Arenz *et al.* has been developed between LEPMI and CEA LITEN. The configuration of the active layer is intermediate between a RDE and a DC of PEMFC, **Figure 1** - B.

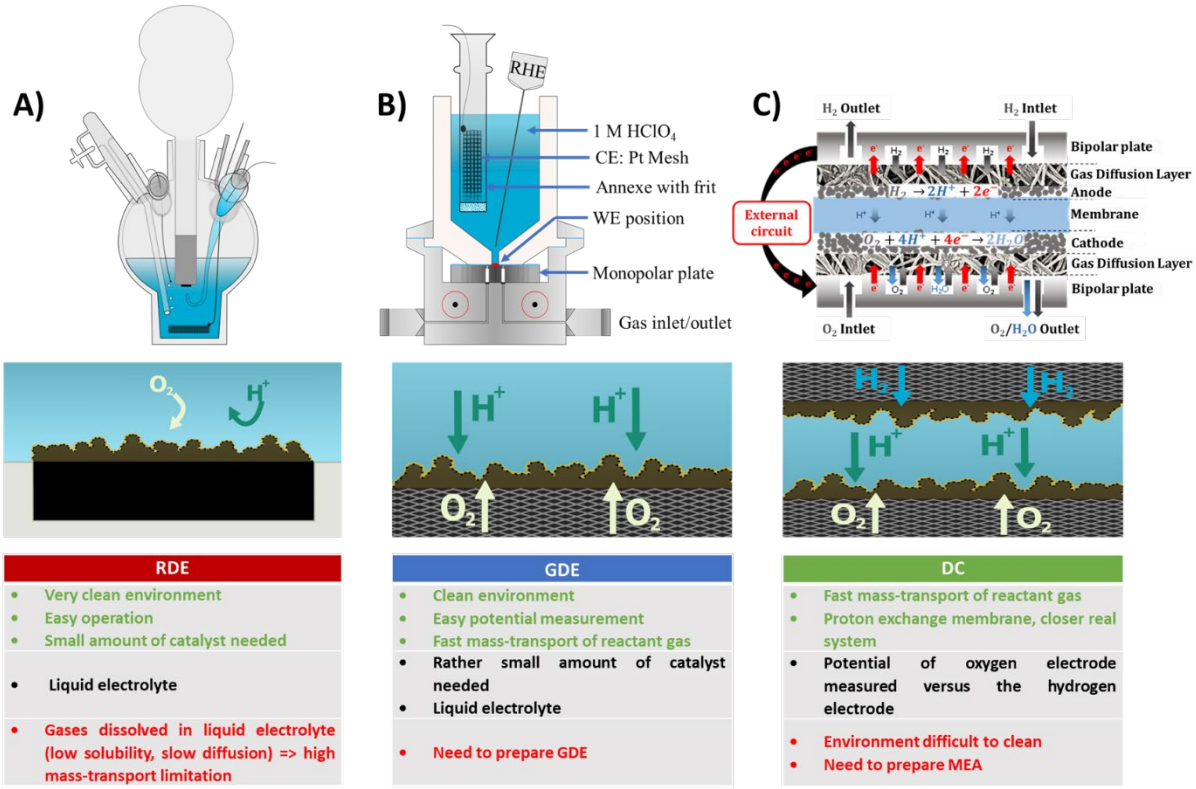

Figure 1: Different schematics of all three kinds of electrode's environments. ***A)*** *RDE,* ***B)*** *GDE and* ***C)*** *DC, and their pros and cons.*

The working electrode has an active surface area of 0.071 cm^2; it is porous and separates the liquid electrolyte (on top), where the counter (placed inside a frit to prevent oxygen bubbles nucleation near the WE) and reference electrodes are located, from the gas reactant phase, a graphite monopolar plate (on the bottom). This configuration has multiple advantages. On the one hand, as for the RDE setup, this configuration enables to have a good control of the electrochemical parameters (the current flow from the working to the counter electrode (platinum mesh), while the potential is precisely controlled/measured using a commercial Reversible Hydrogen Electrode (RHE, Gaskatel). On the other hand, the monopolar plate - baring a flow field of 10 parallel channels pattern of *ca.* 250 µm width (same for lands), enables a flow of oxygen in a similar manner as in a DC (less risk of flooding due to better water removal), thereby strongly enhancing the rate of mass-transport of the gaseous reactant, while protons (and water) shall be easily provided by the liquid electrolyte. The electrolyte was however more concentrated in GDE than in RDE, 1 mol L^{-1} $HClO_4$ aqueous solutions being chosen in GDE experiments, so to avoid/limit proton depletion at the interface in the course of the ORR measurement.

The differential cell used in this work is a small-sized real PEMFC system (1.8 cm^2 geometric active area), with a membrane electrolyte that enables the proton transport from the anode to the cathode while it separates (in theory) the gas reactants. The Pt/C-based negative electrode is operated at high stoichiometry of pure H_2 with a much higher loading than the positive electrode (100 µg cm^{-2} of platinum), so to be considered not limiting, hence

is considered as both a reference and a counter electrode for the positive electrode where the ORR (and hydrogen underpotential deposition, H_{upd}) is performed. It was chosen to operate the DC at 30°C and 100% relative humidity, so to approach the conditions employed in the RDE and GDE (25°C and liquid electrolyte). The cathode loading was kept at 20 µg cm^{-2} of Pt, well below that of the anode (100 µg cm^{-2} of Pt), and the constant gas stoichiometries being very large (*ca.* 50 at 1 A cm^{-2}), so to have at maximum a limitation of the PEMFC performance by the cathode catalyst, and to enable accessing the intrinsic properties of the cathode catalyst at stake, with as little as possible mass transport limitation.

The cathode catalytic inks for both the GDE and DC setups, were prepared by mixing the desired catalyst powder into a solution of ultrapure water (Merck, Direct Q-3UV) and isopropanol (Sigma Aldrich 99.5%) following the same safety measures as for the RDE inks. The solution is then mixed with a magnetic bar for 5 min at 400 rpm and then dispersed using an ultrasonic bath (Elmasonic S15, 35 W, 37 kHz) for 30 min with cold water (after 15 min, the bath water is renewed with cold water). Then the ionomer solution (Nafion D2020) is added, and the final solution is mixed with a magnetic bar overnight at 400 rpm. The catalytic ink is used within 4 days and is kept under mechanical stirring (still at 400 rpm). Before each sampling, the ink is ultrasonicated for 30 min. The precise quantity for each component of the ink is detailed in **Table 1**.

Table 1: Composition of the catalyst inks employed for the MEA preparation.

	TEC10V50E, Pt/XC72	**TEC36V52, PtCo/XC72**	**TEC10EA30E-HT, Pt/GC**
Catalyst (g)	0.5	0.5	0.2
Water (g)	13.9	13.9	13.9
IPA (g)	29	29	29
Ionomer solution (g)	0.8	0.8	0.32
I/C mass ratio	0.7	0.7	0.5

The catalytic ink used for the anode layer is prepared by mixing 2 g TEC10V50E electrocatalyst with 9.25 g of ultrapure water and 0.75 g of ethanol. 30 g of 3 mm diameter zircon beads are then added in the flask and the ink is mixed overnight with a roller mill (IKA roller 10 basic) at 30 rpm at room temperature, as reported by the group of Gasteiger *et al.* [33,34]. The next day, 3.2 g of ionomer solution (Nafion D2020) is added to the vial and the solution is mixed again with the roller mill at 30 rpm all night. All the ink is used on the next day. The same anode was used in all DC experiments, irrespective of the cathode catalyst at stake.

2.4 Catalyst coated membrane fabrication

The cathodic catalytic layers are fabricated by the ultrasonic-spray coating method using an Exactacoat model from Sono-Tek equipped with a 120 kHz Impact nozzle. The spray bench is composed of a nozzle mounted on an arm that can move in 3 dimensions. A syringe filled with the ink allows to dispense the ink until the nozzle. The coating is made on a 250 µm PTFE

sheet that is placed on a vacuum and heating plate set at 80°C. The flow rate is set at 0.08, 0.1 and 0.2 mL min^{-1} for the TEC10V50E, TEC36V52 and TEC10EA30E-HT catalysts, respectively; the *x* and *y* nozzle speeds are fixed at 30 mm s^{-1} and the power at 2 W. The coating consists of 4 serpentine patterns as described in the work of Sassin *et al.* [13]. The loading target is 0.02 mg cm^{-2} of platinum. The real final loading is evaluated by X-ray fluorescence measurements and are 0.019 mg cm^{-2} (±8% of local aerial loading on the elaborated catalyst layer), 0.020 mg cm^{-2} (±8%) and 0.018 mg cm^{-2} (±8%) of platinum for the TEC10V50E, TEC36V52 and TEC10EA30E-HT catalysts, respectively. For the GDE electrodes, the XRF-measured loadings are, following the same order, 0.018 mg cm^{-2} (±7%), 0.020 mg cm^{-2} (±7%) and 0.019 mg cm^{-2} (±8%). The GDE electrodes were subjected to a post-analysis mineralization; the active layers were put into aqua regia in PTFE tubes (CEM), let in open air for 15 minutes and then put to higher temperature and pressure, using a microwave oven (CEM MARS). After a temperature ramp of 5°C min^{-1} to 200°C, the temperature was held for 30 minutes and then the tubes were cooled down to the ambient temperature. The lixiviated solution is then pipetted and diluted in 40 mL of ultra-pure water. The final solution is weighted and further analyzed using an ICP-MS (PerkinElmer NexION 2000) to quantify the amount of platinum that was present on the electrodes tested. The resulting loadings (calculated using the geometric area of the electrodes, 0.071 cm^2) were determined using this technique for all three catalysts studied in this work: 0.021 mg cm^{-2} (±2%), 0.020 mg cm^{-2} (±3%) and 0.018 mg cm^{-2} (±3%). All three electrodes tested for each catalyst were mineralized and the errors presented here are related to the difference between each electrode loading. These loadings were used in the following to determine the mass activity of every catalysts in GDE, and not the XRF measurements, which were however used for DC mass activities calculation.

The anodic catalytic layers are prepared using a doctor blade automatic film coater (Elcometer). The ink is coated on a 250 µm PTFE sheet that is immobilized flat on a vacuum and heating plate set at 60°C. The coating speed is 5 mm s^{-1} and the coating is dried on the heating plate for approximately 5 min. The platinum targeted loading is 0.1 mg cm^{-2}.

Both catalytic layers are then hot-transferred on a Nafion N115 (130 µm thick) membrane for 10 min at 1 MPa and 160°C. The membrane thickness employed was chosen high, so to limit as much as possible the (detrimental) effects of H_2 crossover, that could bias the ECSA and ORR measurements performed at the ORR cathode (these effects are indeed more pronounced for low-loading cathodes like those used herein).

2.5 Electrochemical characterization

2.5.1 RDE and GDE

The electrochemical measurements in liquid environment are done using three (GDE) and four (RDE) electrode cell setups, thermally stabilized at T = 25°C using thermostatic baths and controlled with a Bio-Logic SP-150 or SP300 potentiostat equipped with a frequency analyzer. For each experimental setup, the high frequency resistance is determined at the open circuit potential at 100 kHz with a ±10 mV amplitude. This resistance is then dynamically corrected at 85% and the 15% remaining are post-corrected to access Ohmic-drop corrected (IR-free)

kinetic parameters. In any case, the cell resistance during the experiments was *ca*. 3 to 5 Ω for both the GDE and RDE setups.

For each measurement in RDE, a bubbling period is necessary to saturate the liquid electrolyte with the appropriate gas, prior to every applied electrochemical technique. A rotation of the RDE tip at 400 rpm is maintained as well as a 20 min waiting period for the change in gas saturation of the electrolyte. **Table 2** details the waiting times in RDE and GDE and all the flow rates of gas used in GDE.

Table 2: Time and flow rate of each gas for the RDE (left – in blue) and GDE (right – in red) techniques (liquid electrolyte). The flow rates in RDE are not indicated, but correspond to a few bubbles per second.

	Break-in	CV 20 mV s^{-1}	CO stripping	Pseudo ORR	ORR cycles
Waiting Time (min)	**20 / 10**	**0 / 0**	**5-35 / 3-15**	**0**	**20 / 10**
Gases Flow rate (mL min^{-1})	**50**	**50**	**80**		**60**

To stabilize each electrode, break-in cycles under inert Ar atmosphere are performed with each pristine active layer; this enables to start from a reproducible initial state of surface (reduce the pre-existing platinum oxides and remove/oxidize the organic compounds from their surfaces). The protocol is well acknowledged in the community and consists of 50 cycles of voltammetry in supporting electrolyte within the stability domain of water ($0.05 < E < 1.23$ V *vs.* RHE) with a scan rate of 500 mV s^{-1}. Another sequence of cyclic voltammetry (CV, 3 cycles) is employed for the GDE experiments at 20 mV s^{-1} before the carbon monoxide (CO) stripping protocol.

CO-stripping CVs (see **Figure SI.1** in supplementary information) are used to determine the electrochemical surface area (ECSA) of the Pt-based catalyst in the RDE and GDE configurations. CO is injected to the working electrode while the potential is held at 0.1 V *vs.* RHE for the appropriate amount of time for each setup, which correspond to the waiting period listed in **Table 2**. After a sufficiently long purging time (35 min in RDE and 15 min in GDE), three successive cycles by voltammetry are performed to electrooxidize the CO adsorbed on platinum (first cycle) and then measure the baseline hydrogen adsorption/desorption (H_{upd}) and Pt-oxides formation/reduction characteristics of the given catalyst. To have a similar electrode state, the cyclic voltammetry following the carbon monoxide oxidation cycle is used for the determination of the H_{UPD} related ECSA for GDE and RDE tests as well as for the background subtraction, to remove all the contributions not related to CO oxidation. The electrooxidation charge per surface unit of platinum is taken equal to 420 µC cm^{-2}_{Pt} [35] for every catalyst, knowing that it is not perfectly correct for the Pt_3Co alloy (but is reasonably assumed to remain a correct estimate [36]). For the H_{UPD} ECSA determination, a charge of 210 µC cm^{-2}_{Pt} is considered.

The ORR activity is evaluated by performing slow-scan CVs in O_2 environment (O_2 being either bubbled in the electrolyte – for RDE – or fed through the monopolar plates – for GDE) on the desired catalyst layers. Due to the low ORR current obtained in RDE, a pseudo-ORR is

performed to correct the background (capacitive) current at 5 mV s^{-1} and a rotation speed of 1600 rpm, same conditions used for the evaluation of the ORR activities [9,10]. A 1 min rest period is held at 0.2 V *vs.* RHE to stabilize the current before the voltammetry begins. The same potential range, from 0.2 to 1.05 V *vs.* RHE is used for both the RDE and GDE ORR measurements. 7 cycles are performed for the GDE in order to reach a stable performance (that keep on increasing, until they near-stabilize as the cycles go on) and the determination of the ORR activities is made on the increasing potential scan (positive sweep) of the last cycle (the ORR evaluation is also made on the positive sweep in RDE). For all measurements, a minimum of three samples was used in order to guarantee the reproducibility of the measurements.

2.5.2 Fuel cell operation

The electrochemical characterizations of the CCM are carried out with a FuelCon test bench and a 1.8 cm^2 electrochemical differential cell designed with parallel gas flow channels (of similar design than for the GDE). The MEA is sandwiched between two gas diffusion layers (SGL 22BB) and two 150 µm-thick PTFE gaskets. The electrochemical differential cell allows to work with high stoichiometry in order to guarantee a homogeneous operation in the plane of the catalytic layer.

Prior to any electrochemical tests, a break-in protocol is applied to the MEA. This protocol consists of applying a voltage of 0.1 V for 30 min (for CCM with TEC10V50E and TEC36V52) or 90 min (for CCM with TEC10EA30E-HT) at 80°C under H_2/O_2 flow (38 NL h^{-1} and 18.8 NL h^{-1} respectively), at 80% relative humidity and a total pressure of 1.34 bara (anode and cathode side).

The electrochemical surface area is obtained by cycling the voltage from U = 0.1 V to U = 1.2 V, at 20, 50, 100 and 200 mV s^{-1}, for T = 30°C, 100 % relative humidity, under H_2/N_2 flow (38 NL h^{-1} and 95 NL h^{-1} respectively). It is admitted that the anode is not limiting the system operation, and that cell voltages are (very) close to the potential experienced by the ORR cathode, and hereafter, the DC voltage and cathode potential will be considered similar.

The polarization curves through which the ORR activities are determined are performed at T = 30°C, 100% relative humidity, under H_2/O_2 flow (38 NL h^{-1} and 18.8 NL h^{-1}, respectively) and under atmospheric pressure. A Staircase potentiostatic electrochemical impedance spectroscopy (SPEIS) technique is used instead of cyclic voltammetry in order to obtain a better correction of the Ohmic drop. The procedure is made up of 16 voltage steps of 50 mV maintained for 3 seconds each from U = OCV to U = 0.1 V. At the end of each voltage step, EIS is registered from 50 kHz to 1 kHz; assuming the duration of the EIS measurement, this corresponds to an equivalent voltage sweep rate close to 5 mV s^{-1} (see **Figure SI.2** in supplementary information), which is the sweep rate used in RDE and GDE. 2 cycles of this procedure are carried out and the backward step of the second cycle is used to evaluate the mass and specific activities of the three electrocatalysts. This procedure also enables to have a correction of the high frequency resistance along the “discretized” polarization curve. Indeed this resistance varies while higher current densities are reached; heat and water are

generated, leading to two antagonist modifications of this resistance. The correction of the polarization curve with an adequate point-to-point ohmic drop is similar to an overall correction of a high frequency resistance measured at the OCV, as can be seen on **Figure SI.2**.

As for all the experimental results obtained, the discretization of the DC experiments is made to have a few points to compare in the range of 0.95 to 0.6 V. After correction of the ohmic drop and of the hydrogen crossover, the first experimental point is taken for the highest cell voltage (OCV in DC, closest to 0.95 *vs.* RHE, value of potential that is usually employed to benchmark ORR catalysts in the RDE and GDE characterizations). A linear regression is made for the determination of the points under 0.8 V, as a linear domain is established on the discretized polarization curve obtained with the SPEIS technique. For the value of 0.9 V, a classical linear fit is not relevant, because the electrochemical behavior follows the exponential trend given by the Butler-Volmer equation. A linear regression in a semi-log coordinate system is therefore done using the values measured at the three highest voltages (*ca.* from 0.94 to 0.88 V) with the SPEIS technique to measure the Tafel slopes, for every curve. The ORR activity at 0.9 V is then interpolated from these mean slopes. For all measurements, a minimum of three samples was used in order to guarantee the reproducibility of the measurements.

3 Results and discussion

3.1 Physicochemical properties of the three ORR catalysts

The three ORR catalysts evaluated in this work are commercial and very popular/characterized in the PEMFC community. Here their physicochemical properties were only verified using TEM-XEDS. Representative TEM micrographs are presented for each catalyst on **Figure 2**. The TEC10V50E catalyst (Pt/XC72) consists of small and very agglomerated nanoparticles (in 2D flat rafts at the carbon surface); their high extent of agglomeration likely decreases the effective surface area of the platinum surface. The PtCo/XC72 catalyst (TEC36V52) is made of alloyed PtCo nanoparticles of Pt_3Co atomic average composition, the nanoparticles being essentially round-shaped, isolated (low extent of agglomeration) and of larger diameters than for the Pt/XC72 ones. Finally, the Pt nanoparticles on the graphitized carbon black (TEC10EA30E-HT, Pt/GC) are essentially round-shaped and isolated, with an average particles' diameter that is intermediate between the two other samples. From such representative TEM micrographs, particle size distribution (PSD) histograms have been drawn, based on the isolated nanoparticles only (**Figure 2**). Considering the TEM micrographs, the number-averaged particle size was measured ($\bar{d}_N = \frac{\sum_{i=1}^{n} x_i d_i}{\sum_{i=1}^{n} x_i}$, where x_i is the number of particles having a diameter d_i): it is 2.8, 6.3 and 8.3 nm for the TEC10V50E, TEC10EA30E-HT and TEC36V52, respectively.

The theoretical surfaces areas estimated from these average diameters are *ca*. 100, 44 and 34 $m^2\ g_{Pt}^{-1}$ for the TEC10V50E, TEC10EA30E-HT and TEC36V52, respectively. These values are only calculated from the isolated nanoparticles diameters compiled in the histograms, and this calculation may be significantly biased, because it does not give any weight to the particle's

agglomerates or to the larger nanoparticles which have been detected from TEM but are very awkward to quantify. As a result, the values presented here are a bit higher than those usually encountered in the literature for such catalysts: 2.3 and 4.4 nm for TEC10V50E and TEC10EA30E-HT respectively.

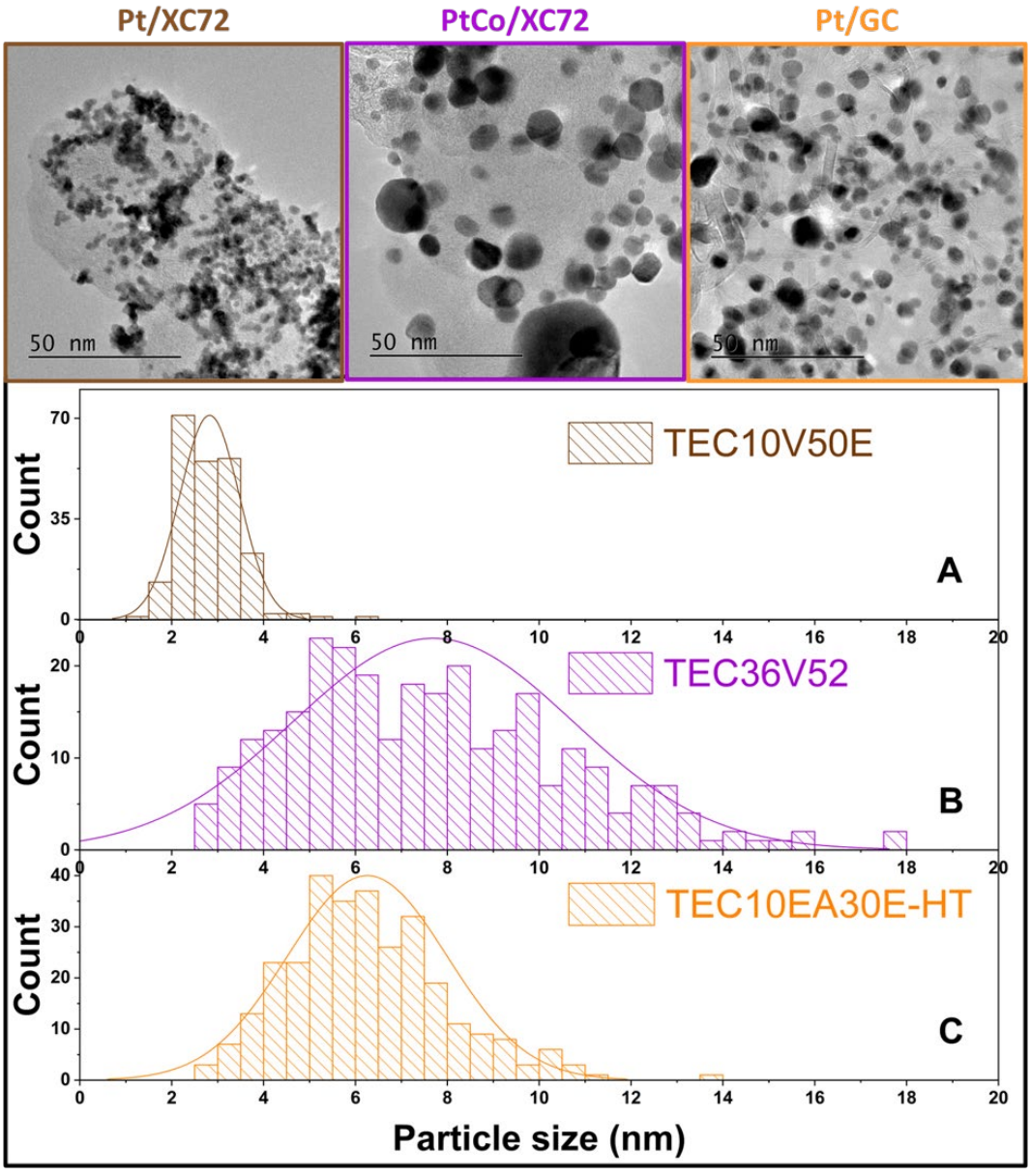

*Figure 2: Representative TEM micrographs and particle size dispersion histograms for isolated nanoparticles of **A)** the TEC10V50E (Pt/XC72, brown), **B)** TEC36V52 (PtCo/XC72, purple) and **C)** TEC10EA30E-HT (Pt/GC, orange) catalysts.*

3.2 Determination of the ECSA: influence of the working electrode environment

This work aims to compare the three experimental devices that are the most used in the literature to benchmark PEMFC cathode catalysts. To that goal, a similar platinum loading has been targeted for all the working electrodes: RDE, GDE or DC and each catalyst at stake. This

catalyst loading is fixed at 20 μg_{Pt} per cm^2 unit area of electrode; such small Pt loading was chosen because it is compatible with the determination of the intrinsic catalytic activity of the chosen catalyst: a small loading shall prevent any "active layer effects", *i.e*. it is not expected that consequent mass-transport limitations occur within the thickness of the active layer, which would be the case in thick active layers [14,37]. Due to a lower loading of the TEC10EA30E-HT, the active layer is expected to be thicker than the two other catalysts, but still thin enough (< 1 µm) to prevent as much as possible these limitations in the thickness of the electrode. The three setups (RDE, GDE and DC) are fundamentally different by the nature of the electrode environments and the way the reactants are fed to the active layer (mass-transport mechanisms of proton, water and oxygen), as well as by the electrochemical control the experimentalist can have on the working electrodes (see **Figure 1**). In particular, these experimental environments induce non-negligible differences with one another when it comes to the evaluation of the electrochemically active surface area (ECSA). For the RDE and GDE, the electrode faces a liquid electrolyte, which can in theory easily access every catalyst particle. The active layer in RDE is likely fully flooded, at least when the catalyst support is not too hydrophobic, which shall be the case for Vulcan XC72 (Pt/XC72 and PtCo/XC72), but is more speculative on a very hydrophobic support like graphitized carbon black (Pt/GC), even if the presence of ionomer can improve the hydrophilicity of the Pt/GC active layer. On the contrary, in the case of the GDE, one side of the active layer is likely flooded (in direct contact with the liquid electrolyte), while the other side of the catalytic layer (on the hydrophobic GDL side) is subjected to a high flow of gas; as a result, one expects that the active layer is (in theory) properly hydrated by the one side and well accessed by the gaseous reactants on the other side. This can of course not perfectly be the case in practice, especially if the active layer is "thick", which shall not be the case for the used catalyst loading (20 μg_{Pt} cm^{-2}). In addition, even if one would consider the GDE configuration in its ideal case, the partial pressure of gaseous species (close to 1 bar for pure gases) should be different from the solubility experienced in liquid electrolyte – and therefore for RDEs, which could modify the equilibrium potentials at stake, notably for hydrogen reactions. In particular, the low vertex potential value applied for H_{UPD} measurements in RDE (0.05 V *vs.* RHE) might not be appropriate to measure the ECSA in the GDE (and DC) configurations, owing to a different HER/HOR equilibrium potential for Pt|gas phase+liquid interface than for a Pt|liquid interface; the upward displacement of the effective potential at which the hydrogen evolution reaction (HER) takes place in GDE (and in PEMFC) [38] may lead to a miscalculation of the ECSA in GDE (and in PEMFC) using the H_{upd} methodology. This will be further discussed hereafter.

Figure 3-A shows that indeed, for a given catalyst (for example the TEC10V50E, Pt/XC72) and the same potential sweep rate values, the shape of the H_{upd} CVs differs a lot between fully flooded active layers (in RDE) and active layers partially in the gas phase (in GDE and DC), incursion to low potentials leading to very large HER currents in the latter cases. In addition, the onset potential for HER is similar for both GDE and DC which leads to two conclusions: (i) the GDE uses a true reference (commercial RHE), which validates that the reference used in DC, meaning the hydrogen electrode, and (ii) the degree of humidification influences this onset potential (having a fully flooded electrode leading to RDE result), which in this case proves the active layer in GDE is not flooded but has rather a similar humidity as the DC. As a

result, the H_{upd} CVs must be performed using a higher low-vertex potential for the GDE and DC, which leads to a non-negligible under-estimation of the ECSA measured from H_{upd} in these cases. The same applies also for the PtCo/XC72. The CO-stripping coulometry is a more reliable technique to measure the ECSA, very similar results being found for the XC72-based active layers in GDE and RDE (**Figure 3**-B, C and **Figure SI.1**). CO-stripping measurements are usually complicated in DC (they are usually not performed in the literature and were not performed herein), and only cyclic voltammetries under H_2/N_2 gas flows are used to determine the ECSA. In any case, one notes the clear underestimation of the ECSA measured with the H_{UPD} in the DC setup experiments, compared to the CO-stripping based ECSA values measured in RDE and GDE. In brief, the ECSA values determined with the CO-stripping technique and the H_{upd} one are within the error bars for RDE but differ significantly for GDE and DC.

Figure 3-B and C also highlight two peculiar issues undergone with the TEC10EA30E-HT (Pt/GC) catalyst, that employs a hydrophobic carbon (graphitized carbon black). The first one is related to the catalyst layer preparation: although the deposition process for the preparation of thin-film RDEs is supposed generate homogeneous and well-dispersed catalyst particles from the ink, it is not satisfactory with the graphitized carbon black (a hydrophobic carbon support). The reproducibility of the ink deposition is uncertain, leading to non-homogeneous and incomplete active layers, presenting areas of thinner (if not absent) active layer, and others of thicker active layer; of course, the local accessibility of the Pt/GC particles differs from one region to the other. The second is connected to the hydrophobic nature of the carbon support, that is therefore less intruded by the liquid electrolyte (especially in the regions of thicker active layer mentioned above). As a result, some regions of the Pt/GC active layer may remain "dry", even in RDE conditions, *i.e*. are not accessible to the liquid electrolyte, giving an underestimation of the ECSA; this applies both to H_{UPD} and CO-stripping characterizations. This effect of underestimation of the ECSA in RDE, clear on Figure 3-B for Pt/GC, is not observed for the other catalysts supported on more hydrophilic carbon (Pt/XC72 and PtCo/XC72), for which the same ECSA is determined via CO-stripping for RDE and GDE (**Figure SI.1**).

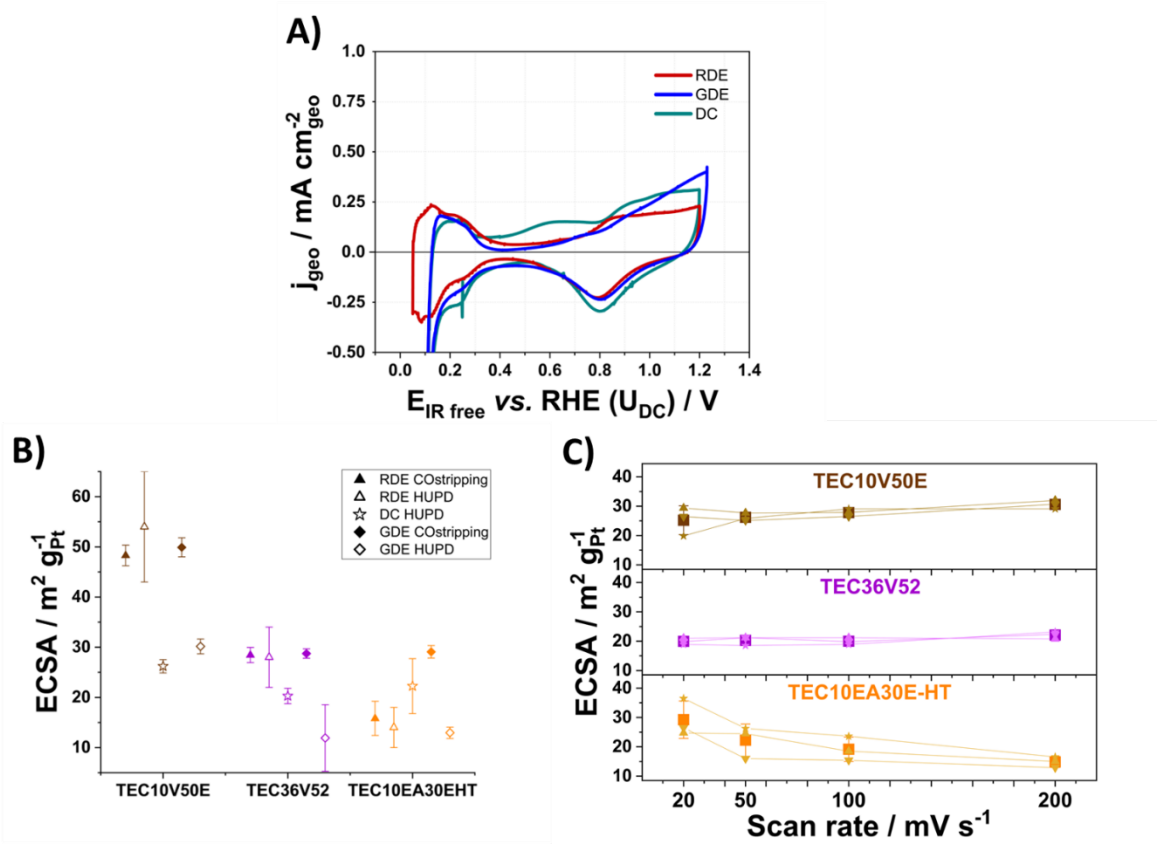

*Figure 3: **A)** CV obtained with Pt/XC72 catalyst under inert atmosphere with the RDE (red), GDE (blue) and DC (green) setups ; **B)** ECSA values determined using CO stripping and H_{upd} methods for the three setups and the three catalysts and **C)** Evolution of the ECSA determined via H_{upd} at different voltage scan rates for the DC setup for Pt/XC72 (brown), PtCo/XC72 (purple) and Pt/GC (orange), the colour code being similar for **B** and **C**.*

Regarding the evolutions of the ECSA measured for all three catalysts as a function of the voltage scan rates (see Figure SI.3 in supplementary information) in the differential cell (**Figure 3**-C), the choice was made to take the values at 50 mV s^{-1}. This choice firstly relies on the fact that a hydrogen oxidation peak appears at the lower vertex potential of the positive scan for higher voltage scan rate (100 and 200 mV s^{-1}), owing to the non-negligible HER witnessed in the negative scan; at high potential scan rate, the evolved H_2 does not have the time to diffuse out of the active layer and some fraction of it can be reoxidized in the subsequent positive sweep. So, taking such data for H_{upd} determination clearly would lead to an over-estimation of the H_{upd} charge (non-negligible bias by some HOR current), and to avoid this, the low vertex potential must be shifted positive by a few mV compared to the case of the RDE (**Figure 3**-A). Secondly, at low scan rate, it is possible that impurities (complex to remove in the PEMFC environment) bias the measurements performed at low potential scan rate (impurities, likely cleaned/displaced at the extreme potentials have the time to diffuse back to the catalytic sites if the potential sweep rate is slow). With this choice of "intermediate" potential sweep rate, the values of active surface for the two Vulcan XC72 supported catalysts do not vary much (**Figure 3**-B); they are still below the values measured by CO-stripping in RDE and GDE, though, but on the same range with the results of H_{UPD} in GDE.

All in all, the ECSAs measured by H_{upd} in DC for the XC72-based catalysts are smaller than the ones made by the CO-stripping method in GDE (the same ink and same deposition process have been used to produce the GDE and DC active layers), which itself is equal to the CO-stripping ECSA made in RDE; it is then reasonable to believe that the DC determination of ECSA is an underestimation of the real surface area, as it has been previously observed for the H_{upd} ECSA measured in GDE versus RDE. On the contrary, the decreased ECSA measured for the graphitized carbon black-supported catalyst (Pt/GC) could be related to the uneven repartition of the water in the active layer volume, leading to proton accessibility issues while increasing the voltage scan rate. In that case, the ECSA measured is monotonically decreasing with the scan rate.

3.3 Determination of the intrinsic ORR activity: influence of the working electrode environment

Knowing their ECSA values, the ORR performance of the three catalysts has been assessed using the three experimental setups (RDE, GDE and DC). The ORR kinetic activity assessment is based on the measured ORR polarization plots in the three setups; the ORR activities have been compared with respect to the Pt loading (mass activity, MA) and to the measured ECSA (by CO-stripping for RDE and GDE and by H_{UPD} at 50 mV s^{-1} for DC, specific activity, SA).

Figure 4 presents a summary of the experimental results obtained for the Pt/XC72 sample (TEC10V50E): the geometric and specific performance of this catalyst is compared in RDE, GDE and DC. A first observation that can be done on these results is that RDE geometric currents of ORR are very significantly inferior to those measured in GDE and DC, owing to the decades larger O_2 mass-transport limitation experienced in liquid electrolyte versus in the gas phase. This is not a surprise and evidently confirms earlier data from colleagues [24,30]. Secondly, one notes the differences in experimental reproducibility (here expressed as error bars on the graphs) from one technique to the other, especially when one compares the GDE and DC: the weight of small heterogeneities on a given sprayed carbon sheet is more important if the working electrodes tested are 0.071 cm^2 samples (GDE) than 1.8 cm^2 samples (DC). In both cases, the geometric current density evolution seems similar at high electrode potential/cell voltages, but a clear separation of the performance measured between the two setups is seen below 0.7 V, at the detriment of the GDE. It is obvious that the latter setup suffers larger mass-transport limitation than the DC at high current densities (low potential), which one can ascribe to water flooding (the GDE is in contact with liquid electrolyte and more water is produced in the catalyst layer at larger current density values), hence to O_2 mass-transport limitation. Indeed, it is unlikely that the limitation occurs by a larger proton transport resistance for the GDE, owing to the fact that (i) there is for sure more liquid water (hence protons) in the GDE setup and (ii) the Nafion ionomer distribution in the DC and GDE active layers should be equal, these active layers being prepared in a similar manner and with similar catalytic ink compositions. So, the O_2 mass-transport limitations are, without any surprise, varying in the order: DC < GDE << RDE, and are essentially occurring by detrimental water flooding of the active layers decreasing in the sequence RDE >> GDE > DC (the water flooding issues being only observed at large current densities/low potential in the case of the GDE).

In addition, the differences of ECSA determination noted previously may lead to a significant gap between the specific current densities (j_{spe}) measured for the RDE and GDE setups (on the one hand) and the DC setup (on the other hand): the higher ORR specific current density at a cell voltage in the range 0.8 to 0.6 V measured for the DC setup, can therefore originate both from a smaller O_2 mass-transport limitation, but also from the fact that the ECSA measured by H_{upd} in this setup is minored compared to that measured by CO-stripping in the GDE (and RDE) setups. Whatever these biases, the Tafel plots representing the specific activities of the Pt/XC72 catalyst measured in these three setups (**Figure 4**-C, bottom) are remarkably superposed in the "medium" potential interval (*i.e*. from 0.9 to 0.8 V *vs.* RHE), which means that any setup is relevant to measure the intrinsic ORR activity of the Pt/XC72 catalyst in these conditions (room temperature, fully hydrated gases or liquid electrolyte, high potential region). The same essentially applies for the mass activities (**Figure 4**-C, top): the mass activities of the TEC10V50E (Pt/XC72) catalyst measured by any of the RDE, GDE or DC setup compare fairly well on the medium potential range investigated, with a non-negligible DC's tendency to underestimate the MA at high cell voltages (explained below).

All the techniques come with their own experimental limitations, though. The Tafel plots show that for high cell voltages/electrode potentials, DC experiments lead to lower current density, being expressed by the catalyst mass (in a pronounced manner) or specific area (in a smaller extent); this effect likely originates from the detrimental H_2 crossover observed in the DC (see **Figure 1**), that negatively shift the open-circuit potential of the cathode in the DC compared to ideal cases where the cathode can be well separated from its counter and reference electrode (GDE and RDE), hence making high potential measurement of the ORR hard to do (the cathode sees some H_2, and the superposed HOR current biases the ORR current, especially around the ORR onset region)[1]. In addition and without surprise, there is no possible measurement of the intrinsic activity for the RDE below 0.8 V *vs.* RHE, while the GDE starts to be severely limited by O_2 mass-transport below 0.7 V *vs.* RHE. Tafel slopes can be calculated using the discretized points from 0.95 to 0.6 V shown on **Figure 4**-C for Pt/XC72 and on the related figures for PtCo/XC72 and Pt/GC. All in all, in the case of Pt/XC72, the values of Tafel slopes in the "high potential region" (*i.e*. from 0.9 to 0.8 V *vs.* RHE) are close to 90 mV dec^{-1} in RDE and GDE, and 64 mV dec^{-1} in DC; those in the low potential region (from 0.8 to 0.6 V *vs.* RHE) are closer to 170 (in DC) and 210 (in GDE) mV dec^{-1}, which is not in agreement with earlier reports on these materials [14,39]. These large values support the assumption that not only charge-transfer kinetics is at stake for all the setups (even with the Koutecky-Levich correction in RDE, and all experimental efforts to limit the mass-transport limitations in GDE and DC).

[1] It has to be noted that the H_2 crossover in DC has a larger impact on the CV measured in H_2/N_2 configuration in the present case (low cathode catalyst loading, 20 μg_{Pt} cm^{-2}) than for usual cathode loadings (> 100 μg_{Pt} cm^{-2}), because in the former case, the small catalyst loading results in small capacitive current in the CV, and therefore to a larger influence of the H_2 crossover current. The same applies for the ORR measurement, in particular close to the OCP (*i.e*. for cathode potentials larger than 0.9 V *vs.* RHE).

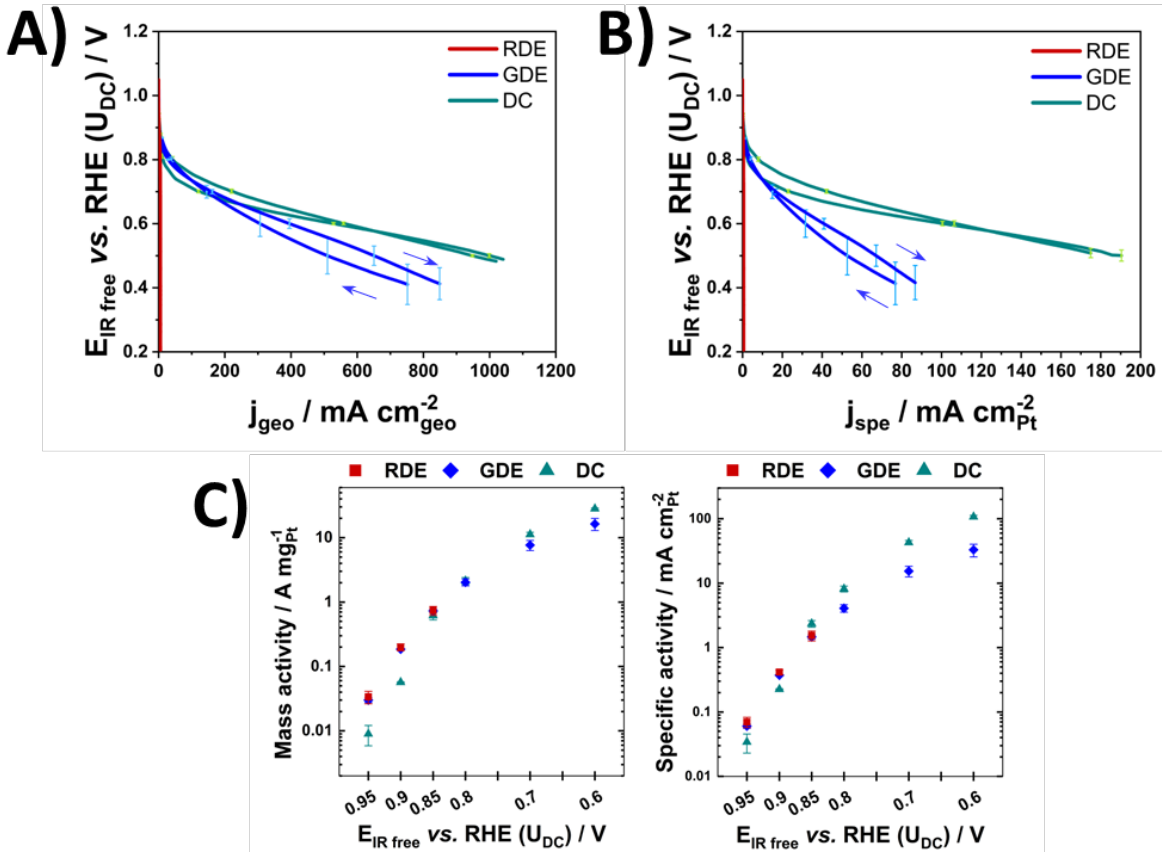

*Figure 4: Experimental results obtained with the TEC10V50E catalyst. **A)** Mean polarization curves with respect to the geometric surface of the electrodes, **B)** Mean polarization curves with respect to the chosen ECSA, **C)** Tafel plots summarizing the mass and specific activities at different potentials and cell voltages. All the graphs contain the results of all three setups studied, with the same color code as for previous figures (RDE in red, GDE in blue and DC in green).*

The trend observed on **Figure 5** for the bimetallic catalyst (PtCo/XC72, TEC36V52) is fairly similar than the one of the Pt/XC72: RDE still presents decades lower geometric current densities than GDE and DC, and a better reproducibility of the results is observed for the DC experiments than for the GDE. Nevertheless, GDE and DC geometric and specific current densities are closer to one another for this alloyed catalyst on the whole range of potential/cell voltage. A higher difference stands out for the specific current density (**Figure 5**-B) as the ECSA is still different for the two sets of experiments, the reason being the same as observed on the CVs (**Figure 5**-D) under inert atmosphere for the H_{UPD} potential region. The ratio between the ECSA determined for the GDE via CO-stripping and for the DC via H_{upd} is *ca.* 1.5, lower than the factor 2 measured between the low potentials' (0.8 to 0.6 V *vs*. RHE) specific current densities for these two setups. The difference noted previously on the ECSA is therefore not sufficient to explain on its own the gap between the specific current density observed in GDE and DC. This corroborates the hypothesis of a non-negligible limitation by the oxygen mass-transport in the case of the GDE, which is therefore not related to the nature of the catalyst (observed for Pt/XC72 and PtCo/XC72). Another possibility that must be considered is the difference in electrode size and the thermal management of the GDE and the DC: the latter having 25 times higher mass of platinum, it will lead to higher currents than in GDE (at a given current density) and then will generate more heat. Contrary to the GDE, the DC has no bulk liquid electrolyte

near the working electrode, so the heat produced (related to the high current generated) results in larger local thermal gradient in the DC (in GDE, the heat can be evacuated in the liquid electrolyte). These heterogeneities in thermal management can have a detrimental impact and lead to experimental discrepancies in measured ORR activities. The Tafel plots also show that the RDE results are not in an as good agreement as has been previously demonstrated with the GDE and DC setups for TEC10V50E in **Figure 4**. At high electrode potentials where RDE can be performed, all the values of activity measured with this technique are below the ones obtained in GDE/DC. This underestimation of the RDE activity cannot be attributed neither to the cleanliness of the setup (DC assumed to be the worst case), nor to the liquid environment (shared with GDE), but of course, it is expected that the mass-transport limitation is more critical for more active catalysts, which is the case for PtCo/XC72 versus Pt/XC72: at given overpotential, oxygen is depleted more rapidly for PtCo/XC72, due to highest current densities per unit surface of material, leading to a lower concentration of reactant at the vicinity of the active site. The evolution of the current density follows a similar logarithmic slope for RDE and GDE, close to 95 mV dec^{-1} and a smaller slope for DC, as reported for Pt/XC72 of *ca.* 75 mV dec^{-1}, but the starting point of the measured activity is not the same. For both "liquid electrolyte" setups, the open circuit potential is yet almost the same (*ca.* 1.06 V *vs.* RHE) and significantly higher than the open circuit voltage in DC (*ca.* 0.945 V, assumed to correspond to 0.945 V *vs.* RHE for the cathode open circuit potential) which should lead to the same activities even for the RDE and GDE experimental setups. The ratio of the GDE versus RDE activity at high electrode potential, being superior to 1, is nonetheless a proof of (i) the cleanliness of the GDE setup (no real poisoning of the catalysts is witnessed) and (ii) the fact that the GDE data can of course be more considered non-mass-transport-limited compared to the RDE data, even after mass-transport correction in the latter case and for rather high electrode potentials. The high potentials Tafel slopes are quite similar to those of the TEC10V50E catalyst, but the slopes in the low potential region are significantly higher, 240 mV dec^{-1}; this value is twice the value expected for the ORR reaction kinetics at such potentials [40], and this shows that the mass-transport limitation is by no mean negligible in these conditions [39], even in the case of the GDE and DC; this is again no surprise, owing to the high ORR activity of the PtCo/XC72 catalyst. Nonetheless, a very good correlation between GDE and DC results is observed for the mass activity and especially for the specific activity measurements on the whole range of potentials. This agrees with the observation on TEC10V50E, and further shows that these setups lead to comparable assessment of the catalytic activity on the whole "useful" cathode potential range of a PEMFC (0.6 – 0.9 V *vs.* RHE).

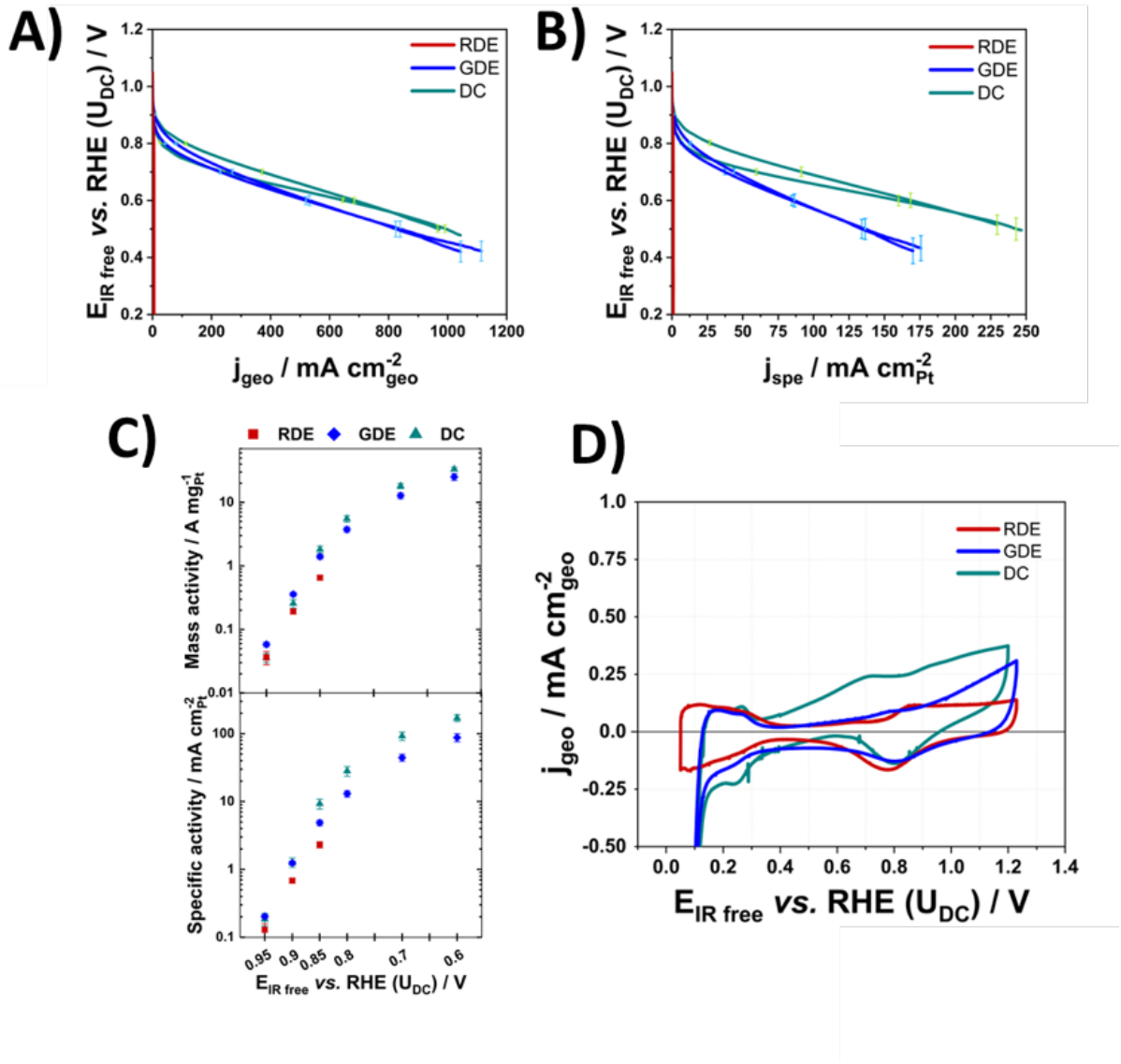

Figure 5: Experimental results obtained with TEC36V52 catalyst. ***A)*** *Mean polarization curves with respect to the geometric surface of the electrodes,* ***B)*** *Mean polarization curves with respect to the chosen ECSA,* ***C)*** *Tafel plots summarizing the mass and specific activities at different potentials and cell voltages and* ***D)*** *CV at 20 mV s^{-1} with respect to the geometric surface of the electrodes. All the graphs contain the results of all three setups studied, with the same color code as for previous figures (RDE in red, GDE in blue and DC in green).*

The PtCo/XC72 catalyst has been studied as it promises a higher intrinsic activity in RDE, but with a real question on the uncertainties to maintain the improvement factor measured at very high electrode potentials in the RDE setup (0.95 and 0.9 V *vs.* RHE) for the "useful" cathode potential range of a PEMFC (0.6 – 0.9 V *vs.* RHE). **Figure 6** presents all the improvement factors (IF) for TEC36V52 and TEC10EA30E-HT, using the same setup, the results for TEC10V50E being the reference for the calculations. **Figure 6**-A and C are related to the specific activity ratios, and **Figure 6**-B and D to the mass activity ratios. For the three different setups, the predicted improvement of PtCo/XC72 seen in RDE at high electrode potentials is maintained in GDE and DC at lower potential values. In fact, the enhancement factors of the PtCo/XC72 catalyst promised in RDE are even better with the other experimental setups. At

lower potential values (and larger current densities) in a close-to-real PEMFC cell, the catalyst still exhibits improved current density, independently on the relevant studied parameters (real surface or mass of catalyst) and this can be assessed as well by GDE measurements. These improvement factors are nearly constant in GDE and vary more for the DC, which suggests a possible change of behavior of either the alloyed or the reference catalyst during the experiment in the DC conditions. The higher IF measured at higher cell voltage can be attributed to the fact that PtCo/XC72 (here composed of rather large nanoparticles, see **Figure 2**) is believed to be less affected by platinum oxides at large potential values than Pt/XC72 (composed of much smaller and more agglomerated nanoparticles). Specific activity is of course useful to understand the ORR kinetics, but the mass activity is of more interest for the cost-related performance, related directly to the quantity of catalyst that has to be integrated in real PEMFC (this is more relevant for industrials). Here, while the mass related IF of PtCo/XC72 is less spectacular than its specific area related IF, it is still way above 1, which confirms the practical (industrial) interest of this catalyst.

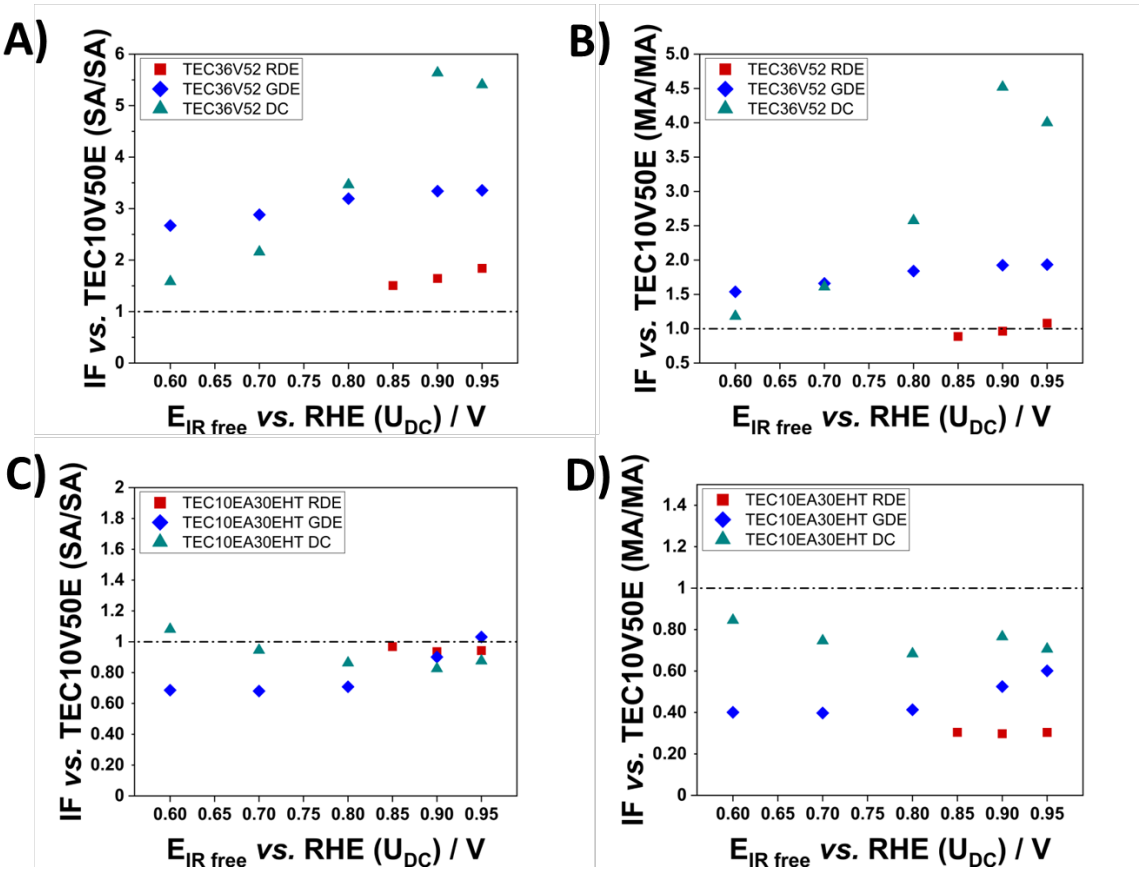

*Figure 6: Improvement factors relative to the TEC10V50E catalyst for all three setups measured via **A)** specific activities and **B)** mass activities ratio for the TEC36V52 catalyst and **C)** specific activities and **D)** mass activities ratio for the TEC10EA30E-HT catalyst.*

Figure 7 explores the case of a platinum catalyst supported a graphitized carbon black (Pt/GC, TEC10EA30E-HT). Although the trend between RDE and GDE/DC characterizations is the same (hugely larger O_2 mass-transport limitation in RDE), non-negligible differences are also witnessed between the GDE and DC for the polarization curves, even in the high potential region. The explanation that is put forth to account for these differences is once again linked

to the water management for both setups, which is believed to be tremendously different for this carbon support. **Figure 7**-B shows that GDE results suffer the same limitation as that observed for TEC10V50E (**Figure 4**). The Pt/GC catalyst presents the lowest maximum geometric current density in GDE (the reproducibility being high for this experimental setup). It reaches the same maximum specific current density, presumably a limitation related to the nature of the catalyst itself, an expected result, but with a very different shape of the upward and downward potential sweeps, which is less present for the Vulcan XC72-supported catalysts. The upward cycle has degraded performance compared to the downward cycle. A period at high potential may have a positive effect on water removal, leading afterward to higher current densities (even though it creates Pt oxides that can have a detrimental effect on the ORR). All these findings point out that environmental issues are present for the GDE experiments of this catalyst, mainly related to the possible flooding of the active layer due to inefficient water removal. In spite of that, **Figure 7**-C displays that RDE and GDE results at high electrode potentials are a good match, as it is the case for TEC10V50E, with also the same issue for the highest potential point.

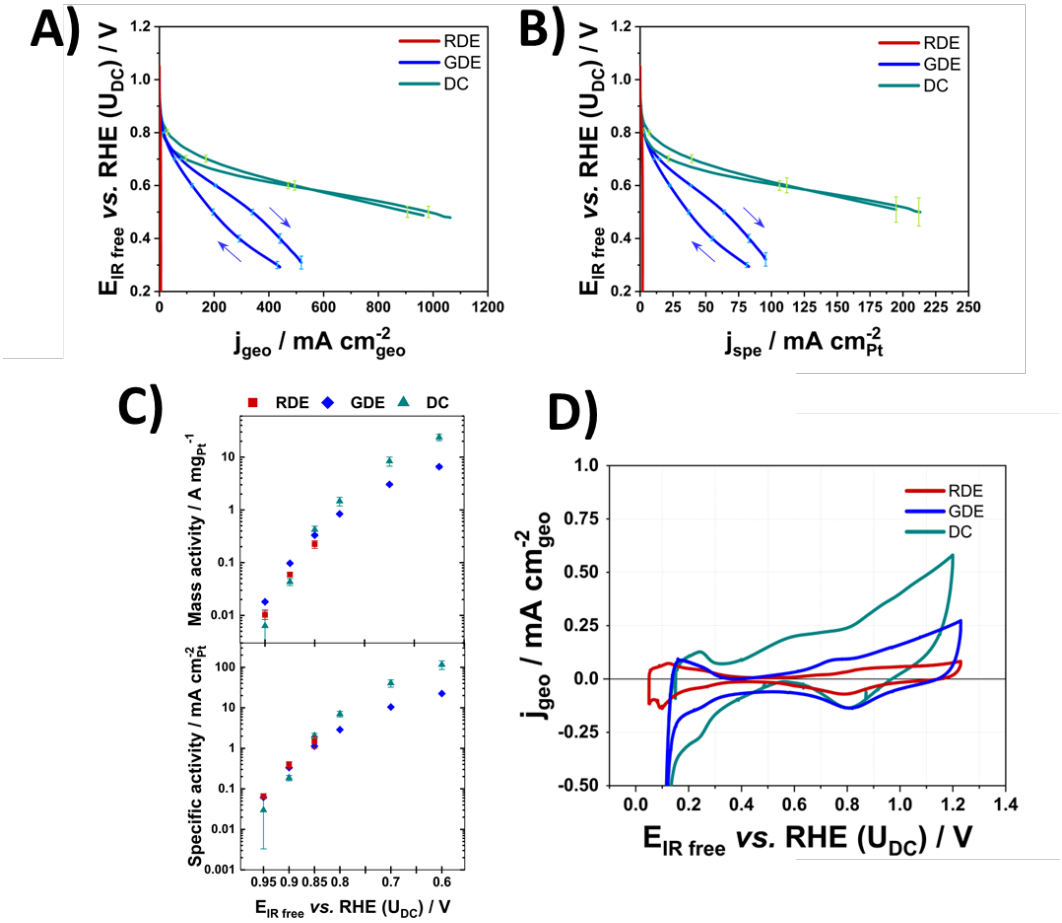

Figure 7: Experimental results obtained for TEC10EA30E-HT catalyst. ***A)*** *Mean polarization curves with respect to the geometric surface of the electrodes,* ***B)*** *Mean polarization curves with respect to the chosen ECSA,* ***C)*** *Tafel plots summarizing the mass and specific results at different potentials and cell voltages and* ***D)*** *CV at 20 mV* s^{-1} *with respect to the geometric surface of the electrodes. All the graphs contain the results of all three setups studied.*

There is a good overlap of the ORR activity results in the potential range of RDE, which once more gives confidence in a possible extrapolation of RDE results to a broader potential range. This good extrapolation seems to have a relation with the nature of the catalyst studied, single metal nanoparticles in this case, more than on the carbon support. The detrimental gap observed for the specific current density in GDE and DC cannot be explained via the difference in ECSA measurement, as the ratio between CO stripping and H_{upd} active surface is, by far, the lowest among all the catalysts studied. **Figure 6** also showed a particular discrepancy between the specific activity of the Pt/VC and Pt/GC. The comparison is not in favor of the latter, as it hardly maintains similar activity. On the contrary, the mass activity is absolutely not the same and falls down for all three setups to half or even a third of the activity obtained with the Pt/VC for GDE and RDE respectively. This tends to highlight another issue encountered by the Pt/GC catalyst: the heterogenous accessibility to the active sites. Looking at the specific activity related improvement factors, one would conclude that the active sites of Pt/GC work similarly as those for the Pt/XC72 catalyst. However, the quantity of working sites may be smaller than expected for this catalyst, as the mass related factors is tremendously lower. This is particularly well shown by the RDE results, exhibiting almost the highest and at the same time without a doubt the lowest improvement factors related respectively to the specific and mass activity. This trend tends to be reduced with the GDE setup and is nearly absent for the DC. This is the order that has already been given for the presence of water, being more detrimental for this catalyst in RDE, GDE and impacting less the catalyst in DC.

Figure 8, related to DC characterizations, offers a good vision on this phenomenon, as it completely erases the gap between both single metal platinum catalysts. A similar behavior is observed on the whole scanned range of cell voltage for these catalysts, offering a good prospective of comparison for similar catalysts composition (in terms of catalytic particles) as it seems to depend mainly on the nature of the metal and not much on the nature of the carbon support. The PtCo alloyed material is not on par with the two others, and its improvement factor over the pure Pt/C samples is significant on the whole polarization curve (from 0.9 to 0.5 V).

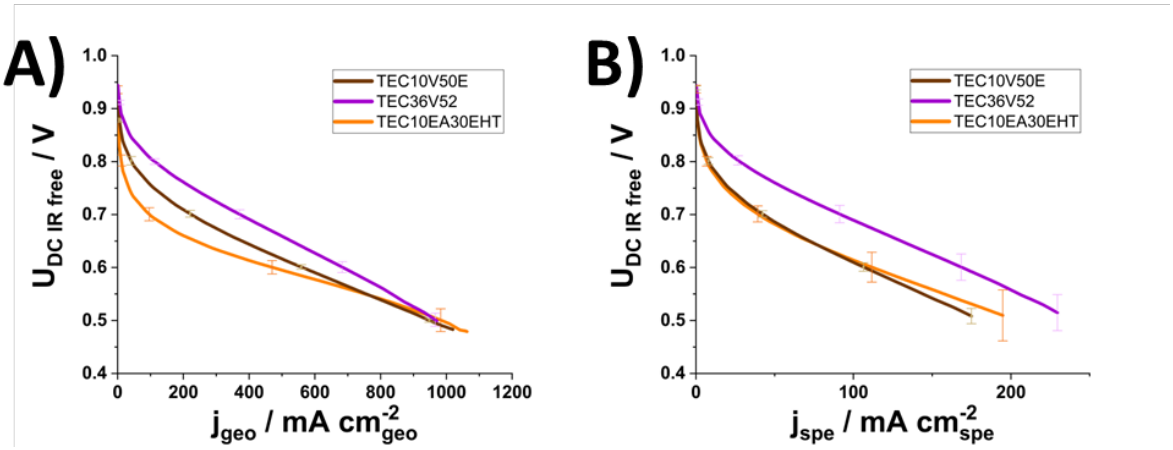

*Figure 8: Mean polarization curves in DC environment for all three catalysts with respect to **A)** the geometric current density and **B)** the specific current density, H_{upd} related ECSA taken at 50 mV s^{-1}.*

3.4 Discussion

This work aimed to compare three of the most used characterization setups of the literature: the Rotating Disk Electrode (RDE), the Gas Diffusion Electrode (GDE) and the Differential Cell (DC) and to check (or not) whether these systems all enable to access the intrinsic (ohmic-drop and mass-transport free) ORR activity of carbon-supported Pt-based catalyst. The considered electrolyte and cell environments, from fully liquid (RDE), to a liquid-gas mix (GDE) and finally to fully-hydrated polymer-gas interface possibly in presence of liquid water (DC), lead to different mass-transport mechanisms for the protons, oxygen and water. Three commercial catalysts were compared, which are all very popular in the PEMFC community, and their intrinsic activities are summarized in **Table 3** for each experimental setup considered (RDE, GDE and DC).

Table 3: Recap chart of all mass (top of the cell) and specific (bottom of the cell) activities for each catalyst and each experimental setup on the whole range of studied potentials

MA (A mg^{-1}_{Pt}) SA (mA cm^{-2}_{Pt})	TEC10V50E			TEC36V52			TEC10EA30E-HT		
Potential	RDE	GDE	DC	RDE	GDE	DC	RDE	GDE	DC
0,95	0.034 ± 0.007 0.07 ± 0.01	0.030 ± 0.003 0.060 ± 0.005	0.009 ± 0.003 0.034 ± 0.011	0.036 ± 0.009 0.13 ± 0.03	0.058 ± 0.005 0.203 ± 0.013	0.036 ± 0.006 0.19 ± 0.04	0.010 ± 0.002 0.066 ± 0.009	0.018 ± 0.001 0.062 ± 0.001	0.006 ± 0.006 0.03 ± 0.03
0,9	0.20 ± 0.02 0.41 ± 0.04	0.186 ± 0.002 0.372 ± 0.006	0.057 ± 0.001 0.226 ± 0.004	0.19 ± 0.02 0.68 ± 0.06	0.36 ± 0.03 1.24 ± 0.09	0.26 ± 0.04 1.3 ± 0.2	0.059 ± 0.006 0.39 ± 0.08	0.098 ± 0.004 0.335 ± 0.009	0.043 ± 0.007 0.19 ± 0.03
0,85	0.7 ± 0.1 1.5 ± 0.3	0.73 ± 0.05 1.5 ± 0.1	0.62 ± 0.09 2.3 ± 0.3	0.65 ± 0.06 2.3 ± 0.2	1.4 ± 0.1 4.9 ± 0.4	1.8 ± 0.2 9.3 ± 1.6	0.22 ± 0.04 1.5 ± 0.5	0.33 ± 0.01 1.14 ± 0.03	0.42 ± 0.07 2.0 ± 0.3
0,8	X	2.0 ± 0.3 4.1 ± 0.5	2.1 ± 0.3 8.2 ± 0.9	X	3.7 ± 0.4 13.0 ± 1.4	5.5 ± 0.7 28.2 ± 4.7	X	0.84 ± 0.04 2.89 ± 0.07	1.5 ± 0.3 7.0 ± 1.1
0,7	X	7.7 ± 1.4 15.4 ± 2.9	11.2 ± 0.8 42.9 ± 3.1	X	12.7 ± 1.3 44 ± 5	18.1 ± 1.7 93 ± 13	X	3.0 ± 0.2 10.5 ± 0.2	8.4 ± 1.7 40.6 ± 8.4
0,6	X	16.4 ± 3.4 32.9 ± 7.3	28.1 ± 0.8 107.4 ± 5.8	X	25.2 ± 3.0 88 ± 12	33.2 ± 2.3 170 ± 20	X	6.6 ± 0.4 22.6 ± 0.6	23.8 ± 3.3 116 ± 28

In each setup, low-loaded electrodes were targeted (20 μg_{Pt} cm^{-2}), to limit as much as possible or ideally suppress the mass-transport limitation in the thickness of the active layer, which should ease the measurement of the materials' intrinsic activity ORR activity. A similar active layer production process was used for the GDE and DC, to avoid any active layer effect

and prevent experimental discrepancies not related to the catalyst itself: the same spray technique was used for the active layers' elaboration, with the same ink formulation recipe and protocol, to have the same particle dispersion, distribution of protonic conducting ionomer in the active layer and the most adapted process (catalyst coated backing for GDE and hot-transfer on membrane for DC). The results obtained showed that each setup has its own peculiarities (advantages and drawbacks), and these may depend on the nature of the catalysts investigated.

The hydrophobicity of the catalyst is an important parameter to be considered, as it strongly influences its interactions with the environment, in particular in presence of liquid electrolyte. This is mainly observed for the interaction of Pt/GC within the RDE liquid electrolyte configuration: the ECSA determination is trickier for Pt/GC than for the two Vulcan XC72-supported catalysts (not same value for CO and H_{upd} ECSAs in RDE), because aggregates of Pt/GC + ionomer may be surrounded but not intruded by liquid water, leading to smaller than expected ECSA in liquid electrolyte (especially in RDE and to some extent GDE). The effect is also somewhat detrimental in DC, the geometric ORR current density being smaller than expected, owing to difficulties for O_2 to reach the core of these aggregates, hence depreciating the measured mass activity.

The high gas flows used to remove all traces of oxygen from the cathode side of the gas diffusion electrodes (GDE and DC) to prevent any oxygen reduction current for a clean integration of the H_{upd} region implies a thermodynamical displacement of the equilibrium potential of the HOR/HER (the activity of protons and hydrogen is not the same in the gas-ionomer phase than in liquid-electrolyte-ionomer phase), leading to higher hydrogen evolution reaction current at similar electrode potential (*vs.* RHE) / cell voltage around 130 mV, compared to 50 mV *vs.* RHE in the case of a RDE. As a result of this, the CV to measure H_{upd} in GDE and DC must be plotted with a more positive value of the lower vertex potential than in RDE (otherwise, the CV is significantly biased by HER/HOR currents), which renders very questionable the ECSA determination (at the higher low-vertex potential in GDE and DC, one is not sure to complete the H_{upd} layer). So, the H_{udp} methodology may underestimate the ECSA measured in GDE and DC. CO-stripping gives a much more reproducible ECSA evaluation between RDE and GDE, but is usually awkward in DC (and was not performed here). In the end, it was chosen to evaluate the ECSA of the three catalysts by CO-stripping (RDE and GDE) and H_{upd} at 50 mV s^{-1} (DC), choices which are believed to be the "lesser incorrect" to establish a fair comparison of these materials in this study.

The current densities with respect to the geometric and specific surfaces were studied on the relevant range of potentials for the RDE, GDE and DC setups. Because each setup comes with its advantages and drawbacks, the range of potentials where the measurements can be performed may vary from one setup to the other.

- RDE. The mass-transport kinetics of oxygen is much slower in liquid electrolyte, due to the small solubility and diffusivity of oxygen in the liquid electrolyte. This prevents any measurement of the ORR activity below 0.85 V *vs.* RHE in RDE, because the current density is fully mass-transport limited and cannot be corrected. So RDE measurements of the ORR activity are only viable in the range 0.85 – 0.95 V *vs.* RHE.

- GDE. Having O_2 gas that can diffuse from the back side of the GDE (the front side being in contact with the liquid electrolyte) enables to promote much faster mass-transport in the GDE than in the RDE case. ORR kinetics can be more reliably measured in the full range of relevant potential of a PEMFC cathode: 0.6 – 0.95 V *vs.* RHE. However, flooding of the active layer might still occur, especially at large current densities.
- DC. The DC is hindered by the unavoidable H_2 crossover, that results in smaller OCV than in the two previous setups and prevents reliable measurements of the ORR activities above 0.9 V *vs.* RHE. However, below this potential/cell voltage value, the mass-transport is faster than in the previous cases, leading to (usually) better performance, especially at very high current densities/low cell voltage/cathode potential.

Following the work of Ly *et al.* [7], it was feared that the improvement factor observed in RDE for the PtCo/VC electrocatalyst (*ca.* 1.5-2 over the Pt/XC72 electrocatalyst) was expected to fall down to lower extent in GDE and especially in DC. However, the results presented here showed that an even higher improvement factor is observed for the two latter experimental setups, respectively 3 and 4 in average on the potential range of RDE. This shows that the disappointing results shown by Ly *et al.* (coming from many groups on the planet), *i.e*. PEMFC performance being largely lower than anticipated from the RDE predictions, are not explained by the fact the RDE measures an artificially-high intrinsic activity that is not reproduced in PEMFC, but rather that the worse performances in PEMFC originate from electrode effects and not to catalysts effect. Herein, by using on purpose very low-loaded Pt-based active layers, full hydration and high O_2 stoichiometries in GDE and DC, the mass-transport issues that are usual in real PEMFC conditions (from H^+ and/or O_2 transport) are not so encountered, and the intrinsic activity of the catalysts can be measured appropriately. This leaves hope that, with proper PEMFC electrode engineering, advanced ORR catalysts will be successfully used in PEMFC cathodes.

4. Conclusion

This work compared the Rotating Disk Electrode (RDE), the Gas Diffusion Electrode (GDE) and the Differential Cell (DC) to measure the intrinsic (ohmic-drop and mass-transport free) ORR activity of popular carbon-supported Pt-based catalyst. The differences in specific and mass activities observed are related to the fundamental nature of each setup. On the one hand, the RDE enables high cleanness in the measurements and operation with minimal amounts of catalyst material, but is very limited by mass-transport, leading to a partial determination of the intrinsic activities of the catalyst on a restricted part of the studied potential range, but much appropriate for high electrode potentials. On the other hand, GDE is less clean than RDE but much more than DC and is less limited by mass-transport than RDE, enabling the study to lower potential, accessing the range of interest for PEMFC function (0.85 to 0.6V). For the DC, although it is limited by the hydrogen crossover and (possibly) short-circuit currents and suffers from a low cleanliness, which renders difficult high ORR potential measurements, it works in high stoichiometry conditions, the pressure can be regulated to

have better water removal and is more adapted for low cell voltage operation. So, all these systems have their own advantages and drawbacks.

They all enable a meaningful comparison of state-of-the-art carbon-supported Pt-based catalysts, and the study shows that the improvement factors observed in RDE are essentially maintained in GDE and DC, at least if the gas diffusion electrodes (catalyst layers) are prepared in the same way.

Finally, this study highlights the possibility to compare the results obtained in RDE to those obtained in GDE and DC, at least until 0.8 V vs. RHE, regardless of the nature of the catalyst considered (within the ones studies herein). The GDE appears as a nice intermediate tool between the RDE and DC, enabling high current density measurements with low platinum loading and without requiring the use of important amounts of catalyst powder or of a complex and costly lab auxiliary as the one needed for DC tests. However, it remains to study the possibility of carrying out measurements at higher temperature. Finally, the DC is a very useful tool to investigate more in detail all the issue related to the integration of complex catalysts, such as the ink formulation and its effect on the electrode performance; it is therefore a nice complement to the RDE and GDE to tailor active layers/electrodes for practical applications.

Acknowledgements

The authors would like to thank Pascal Martin from CEA Grenoble for his contribution to the development and production of the gas diffusion electrode cell's schematics and his expertise in CA Design. MC and RR thank Matthias Arenz for gratefully welcoming students to Univ. Bern, and for having provided an original version of the schematics and a cell of his GDE setup for the preliminary tests to LEPMI. RR, CL and MC also thank Vincent Martin for his great help for ICP-MS measurements, Arnaud Viola and Camille Roiron for fruitful discussions about Microwaves digestions, and Marie Heitzmann and Jean-François Blachot (CEA Grenoble) for their support in the project. This work was supported by funds for the CARNOT Energies du Futur (OPTIPEM project), as well as funding from CEA Grenoble (for the PhD thesis of FV) and from Symbio (for the PhD thesis of RR). Some of this work has been performed within the framework of the Centre of Excellence of Multifunctional Architectured Materials (CEMAM), Grenoble France n◦ ANR-10-LABX-44–01.

Authors' Contribution

RR, FV, CL performed all the electrochemical experiments. MC performed the TEM analyses. All authors analyzed the data and reviewed the contribution, which has been first drafted by RR and CL. MC conceptualized the study.

Consent for publication

The authors declare that they consent to the publication of this paper

Availability of data and material

The data supporting this paper is available within the manuscript and its supporting information

Bibliography

[1] A.F. Ghoniem, Needs, resources and climate change: Clean and efficient conversion technologies, Progress in Energy and Combustion Science. 37 (2011) 15–51. https://doi.org/10.1016/j.pecs.2010.02.006.

[2] A European Green Deal, European Commission - European Commission. (n.d.). https://ec.europa.eu/info/strategy/priorities-2019-2024/european-green-deal_en (accessed October 7, 2022).

[3] P.C.K. Vesborg, T.F. Jaramillo, Addressing the terawatt challenge: scalability in the supply of chemical elements for renewable energy, RSC Adv. 2 (2012) 7933–7947. https://doi.org/10.1039/C2RA20839C.

[4] W. Vielstich, A. Lamm, H.A. Gasteiger, eds., Handbook of fuel cells, Wiley, Chichester, England ; New York, 2003.

[5] H.A. Gasteiger, W. Vielstich, H. Yokokawa, eds., Handbook of fuel cells, John Wiley & Sons, Ltd, Chichester, 2009.

[6] R. Chattot, O. Le Bacq, V. Beermann, S. Kühl, J. Herranz, S. Henning, L. Kühn, T. Asset, L. Guétaz, G. Renou, J. Drnec, P. Bordet, A. Pasturel, A. Eychmüller, T.J. Schmidt, P. Strasser, L. Dubau, F. Maillard, Surface distortion as a unifying concept and descriptor in oxygen reduction reaction electrocatalysis, Nature Mater. 17 (2018) 827–833. https://doi.org/10.1038/s41563-018-0133-2.

[7] A. Ly, T. Asset, P. Atanassov, Integrating nanostructured Pt-based electrocatalysts in proton exchange membrane fuel cells, Journal of Power Sources. 478 (2020) 228516. https://doi.org/10.1016/j.jpowsour.2020.228516.

[8] I. Takahashi, S.S. Kocha, Examination of the activity and durability of PEMFC catalysts in liquid electrolytes, Journal of Power Sources. 195 (2010) 6312–6322. https://doi.org/10.1016/j.jpowsour.2010.04.052.

[9] Y. Garsany, I.L. Singer, K.E. Swider-Lyons, Impact of film drying procedures on RDE characterization of Pt/VC electrocatalysts, Journal of Electroanalytical Chemistry. 662 (2011) 396–406. https://doi.org/10.1016/j.jelechem.2011.09.016.

[10] Y. Garsany, J. Ge, J. St-Pierre, R. Rocheleau, K.E. Swider-Lyons, Analytical Procedure for Accurate Comparison of Rotating Disk Electrode Results for the Oxygen Reduction Activity of Pt/C, J. Electrochem. Soc. 161 (2014) F628–F640. https://doi.org/10.1149/2.036405jes.

[11] S.S. Kocha, Principles of MEA preparation, in: Handbook of Fuel Cells, Vielstich, W.; Lamm, A.; Gasteiger, H. A., Wiley, Chichester, 2003: pp. 538–565. https://doi.org/10.1002/9780470974001.f303047.

[12] R. Makharia, S. Kocha, P. Yu, M.A. Sweikart, W. Gu, F. Wagner, H.A. Gasteiger, Durable PEM Fuel Cell Electrode Materials: Requirements and Benchmarking Methodologies, ECS Trans. 1 (2006) 3–18. https://doi.org/10.1149/1.2214540.
[13] M.B. Sassin, Y. Garsany, B.D. Gould, K.E. Swider-Lyons, Fabrication Method for Laboratory-Scale High-Performance Membrane Electrode Assemblies for Fuel Cells, Anal. Chem. 89 (2017) 511–518. https://doi.org/10.1021/acs.analchem.6b03005.
[14] O. Antoine, R. Durand, RRDE study of oxygen reduction on Pt nanoparticles inside Nafion: H2O2 production in PEMFC cathode conditions, Journal of Applied Electrochemistry. 30 (2000) 839–844. https://doi.org/10.1023/A:1003999818560.
[15] O. Antoine, Y. Bultel, R. Durand, Oxygen reduction reaction kinetics and mechanism on platinum nanoparticles inside Nafion®, Journal of Electroanalytical Chemistry. 499 (2001) 85–94. https://doi.org/10.1016/S0022-0728(00)00492-7.
[16] Y. Bultel, L. Genies, O. Antoine, P. Ozil, R. Durand, Modeling impedance diagrams of active layers in gas diffusion electrodes: diffusion, ohmic drop effects and multistep reactions, Journal of Electroanalytical Chemistry. 527 (2002) 143–155. https://doi.org/10.1016/S0022-0728(02)00835-5.
[17] J. Bett, K. Kinoshita, K. Routsis, P. Stonehart, A comparison of gas-phase and electrochemical measurements for chemisorbed carbon monoxide and hydrogen on platinum crystallites, Journal of Catalysis. 29 (1973) 160–168. https://doi.org/10.1016/0021-9517(73)90214-5.
[18] P. Stonehart, P.N. Ross, The use of porous electrodes to obtain kinetic rate constants for rapid reactions and adsorption isotherms of poisons, Electrochimica Acta. 21 (1976) 441–445. https://doi.org/10.1016/0013-4686(76)85123-7.
[19] C.M. Zalitis, D. Kramer, A.R. Kucernak, Electrocatalytic performance of fuel cell reactions at low catalyst loading and high mass transport, Phys. Chem. Chem. Phys. 15 (2013) 4329. https://doi.org/10.1039/c3cp44431g.
[20] C.M. Zalitis, J. Sharman, E. Wright, A.R. Kucernak, Properties of the hydrogen oxidation reaction on Pt/C catalysts at optimised high mass transport conditions and its relevance to the anode reaction in PEFCs and cathode reactions in electrolysers, Electrochimica Acta. 176 (2015) 763–776. https://doi.org/10.1016/j.electacta.2015.06.146.
[21] C. Jackson, L.F.J.M. Raymakers, M.J.J. Mulder, A.R.J. Kucernak, Assessing electrocatalyst hydrogen activity and CO tolerance: Comparison of performance obtained using the high mass transport ‘floating electrode’ technique and in electrochemical hydrogen pumps, Applied Catalysis B: Environmental. 268 (2020) 118734. https://doi.org/10.1016/j.apcatb.2020.118734.
[22] C. Jackson, X. Lin, P.B.J. Levecque, A.R.J. Kucernak, Toward Understanding the Utilization of Oxygen Reduction Electrocatalysts under High Mass Transport Conditions and High Overpotentials, ACS Catal. 12 (2022) 200–211. https://doi.org/10.1021/acscatal.1c03908.
[23] G.K.H. Wiberg, M. Fleige, M. Arenz, Gas diffusion electrode setup for catalyst testing in concentrated phosphoric acid at elevated temperatures, Review of Scientific Instruments. 86 (2015) 024102. https://doi.org/10.1063/1.4908169.
[24] B.A. Pinaud, A. Bonakdarpour, L. Daniel, J. Sharman, D.P. Wilkinson, Key Considerations for High Current Fuel Cell Catalyst Testing in an Electrochemical Half-Cell, J. Electrochem. Soc. 164 (2017) F321–F327. https://doi.org/10.1149/2.0891704jes.

[25] M. Inaba, A.W. Jensen, G.W. Sievers, M. Escudero-Escribano, A. Zana, M. Arenz, Benchmarking high surface area electrocatalysts in a gas diffusion electrode: measurement of oxygen reduction activities under realistic conditions, Energy Environ. Sci. 11 (2018) 988–994. https://doi.org/10.1039/C8EE00019K.
[26] S. Alinejad, J. Quinson, J. Schröder, J.J.K. Kirkensgaard, M. Arenz, Carbon-Supported Platinum Electrocatalysts Probed in a Gas Diffusion Setup with Alkaline Environment: How Particle Size and Mesoscopic Environment Influence the Degradation Mechanism, ACS Catal. 10 (2020) 13040–13049. https://doi.org/10.1021/acscatal.0c03184.
[27] J. Schröder, J. Quinson, J.K. Mathiesen, J.J.K. Kirkensgaard, S. Alinejad, V.A. Mints, K.M.Ø. Jensen, M. Arenz, A New Approach to Probe the Degradation of Fuel Cell Catalysts under Realistic Conditions: Combining Tests in a Gas Diffusion Electrode Setup with Small Angle X-ray Scattering, J. Electrochem. Soc. 167 (2020) 134515. https://doi.org/10.1149/1945-7111/abbdd2.
[28] K. Ehelebe, D. Seeberger, M.T.Y. Paul, S. Thiele, K.J.J. Mayrhofer, S. Cherevko, Evaluating Electrocatalysts at Relevant Currents in a Half-Cell: The Impact of Pt Loading on Oxygen Reduction Reaction, J. Electrochem. Soc. 166 (2019) F1259–F1268. https://doi.org/10.1149/2.0911915jes.
[29] K. Ehelebe, J. Knöppel, M. Bierling, B. Mayerhöfer, T. Böhm, N. Kulyk, S. Thiele, K.J.J. Mayrhofer, S. Cherevko, Platinum Dissolution in Realistic Fuel Cell Catalyst Layers, Angew. Chem. Int. Ed. 60 (2021) 8882–8888. https://doi.org/10.1002/anie.202014711.
[30] K. Ehelebe, N. Schmitt, G. Sievers, A.W. Jensen, A. Hrnjić, P. Collantes Jiménez, P. Kaiser, M. Geuß, Y.-P. Ku, P. Jovanovič, K.J.J. Mayrhofer, B. Etzold, N. Hodnik, M. Escudero-Escribano, M. Arenz, S. Cherevko, Benchmarking Fuel Cell Electrocatalysts Using Gas Diffusion Electrodes: Inter-lab Comparison and Best Practices, ACS Energy Lett. 7 (2022) 816–826. https://doi.org/10.1021/acsenergylett.1c02659.
[31] T. Lazaridis, B.M. Stühmeier, H.A. Gasteiger, H.A. El-Sayed, Capabilities and limitations of rotating disk electrodes versus membrane electrode assemblies in the investigation of electrocatalysts, Nat Catal. 5 (2022) 363–373. https://doi.org/10.1038/s41929-022-00776-5.
[32] C.C. Herrmann, G.G. Perrault, A.A. Pilla, Dual reference electrode for electrochemical pulse studies, Anal. Chem. 40 (1968) 1173–1174. https://doi.org/10.1021/ac60263a011.
[33] A. Orfanidi, P. Madkikar, H.A. El-Sayed, G.S. Harzer, T. Kratky, H.A. Gasteiger, The Key to High Performance Low Pt Loaded Electrodes, J. Electrochem. Soc. 164 (2017) F418–F426. https://doi.org/10.1149/2.1621704jes.
[34] A. Orfanidi, P.J. Rheinländer, N. Schulte, H.A. Gasteiger, Ink Solvent Dependence of the Ionomer Distribution in the Catalyst Layer of a PEMFC, J. Electrochem. Soc. 165 (2018) F1254–F1263. https://doi.org/10.1149/2.1251814jes.
[35] Warsaw University, Department of Chemistry, Pasteura 1, 02-093 Warsaw, Poland, M. Łukaszewski, Electrochemical Methods of Real Surface Area Determination of Noble Metal Electrodes – an Overview, Int. J. Electrochem. Sci. (2016) 4442–4469. https://doi.org/10.20964/2016.06.71.
[36] L. Dubau, F. Maillard, M. Chatenet, J. André, E. Rossinot, Nanoscale compositional changes and modification of the surface reactivity of Pt3Co/C nanoparticles during proton-exchange membrane fuel cell operation, Electrochimica Acta. 56 (2010) 776–783. https://doi.org/10.1016/j.electacta.2010.09.038.

[37] F. Gloaguen, F. Andolfatto, R. Durand, P. Ozil, Kinetic study of electrochemical reactions at catalyst-recast ionomer interfaces from thin active layer modelling, Journal of Applied Electrochemistry. 24 (1994) 863–869. https://doi.org/10.1007/BF00348773.
[38] J. Durst, C. Simon, F. Hasché, H.A. Gasteiger, Hydrogen Oxidation and Evolution Reaction Kinetics on Carbon Supported Pt, Ir, Rh, and Pd Electrocatalysts in Acidic Media, J. Electrochem. Soc. 162 (2015) F190–F203. https://doi.org/10.1149/2.0981501jes.
[39] H.A. Gasteiger, S.S. Kocha, B. Sompalli, F.T. Wagner, Activity benchmarks and requirements for Pt, Pt-alloy, and non-Pt oxygen reduction catalysts for PEMFCs, Applied Catalysis B: Environmental. 56 (2005) 9–35. https://doi.org/10.1016/j.apcatb.2004.06.021.
[40] A. Damjanovic, V. Brusic, Electrode kinetics of oxygen reduction on oxide-free platinum electrodes, Electrochimica Acta. 12 (1967) 615–628. https://doi.org/10.1016/0013-4686(67)85030-8.